Evaluation of Different Tools of Precision Finishing for Cold Extruded Sun Gear With Internal-External Tooth Shapes

Zuofa Liu (zuofaliu@163.com)
Chongqing University https://orcid.org/0000-0002-7694-2139
Xi Wang
Wenjie Feng
Jie Zhou
Zhiyuan Qu
Qiang Liang

Research Article

Keywords: Sun gear, internal external tooth shapes, precision finishing, cold extrusion, FE prediction, gear accuracy

Posted Date: March 15th, 2021

DOI: https://doi.org/10.21203/rs.3.rs-288279/v1

Evaluation of different tools of precision finishing for cold extruded sun gear with internal-external tooth shapes

Zuofa Liu [a], Xi Wang [a], Wenjie Feng [b]*, Jie Zhou [a]*, Zhiyuan Qu [a], Qiang Liang [c]

[a] College of Materials Science and Engineering, Chongqing University, Chongqing 400044, China

[b] College of Mechanical Engineering, Chongqing University of Technology, Chongqing 400054, China

[c] College of Mechanical Engineering, Chongqing Technology and Business University, Chongqing, 400060, China

Corresponding author:

Email: wjfeng@cqut.edu.cn (WJ Feng), zhoujie@cqu.edu.cn (J Zhou)

Abstract: Due to the complex metal flow in the cold extrusion of sun gear, the teeth accuracy of formed sun gear is poor. In order to improve the accuracy of the extruded sun gear, a novel precision finishing method with different tools was proposed in this study. Finite element simulations were performed using DEFORM, and a new finite element (FE) prediction strategy was developed to obtain an in-depth understanding of the deviation distribution laws of the finished sun gear. Then, the influences of different finishing tools on tooth deformation, tool stress, forming load and tooth accuracy were examined. The investigation results show that the profile accuracy of external gear can be improved from ninth to seventh class, lead accuracy can be enhanced from tenth to eighth class, and total *M* value deviation of internal spline is reduced to 72.3 μm by the precision finishing method with interference mandrel. Therefore, the interference mandrel is recommended as the optimal reshaping tool for commercial production of sun gears. The simulation results are well agreed with the experimental results, which verifies the feasibility of the precision finishing method and the reliability of the FE prediction strategy.

Key words: Sun gear; internal-external tooth shapes; precision finishing; cold extrusion; FE prediction; gear accuracy

List of symbols

$f_{\alpha i}$	Single profile deviation of finished external gear (i=1~9)
F_{α}	Total profile deviation of finished external gear
T_t	Half tooth thickness of target external gear
T_{Li}	Half tooth thickness of left flank of finished external gear (i=1~9)
T_{Ri}	Half tooth thickness of right flank of finished external gear (i=1~9)
$f_{\beta Li}$	Single helix deviation of left flank of finished external gear (i=1~9)
$f_{\beta Ri}$	Single helix deviation of right flank of finished external gear (i=1~9)
F_{β}	Total helix deviation of finished external gear
Q	Accuracy grade of external gear
M_i	M value of finished internal spline (i=1~9)
M_t	M value of target internal spline
f_{Mi}	Single M value deviation of finished internal spline (i=1~9)
F_M	Total M value deviation of finished internal spline

1. Introduction

As a classical power transmission part, sun gear with internal-external tooth shapes has been widely used in truck transmission systems because of its high transmission accuracy, long service life and reliable operation. Compared with the traditional cutting gears, gears formed by forging and extrusion technologies have the advantage of improved strength teeth in high material utilization and high production efficiency. In recent years, considerable progress has been achieved on spur gears formed by forging or extrusion process. Song, Im [1] presented the process design system for cold forward extrusion of cylindrical gears. They concluded that the extrusion force obtained from the proposed system was essentially in agreement with experimental results. Choia, Choi [2] developed the two-step precision forging

process of spur gears. They found that the forging pressure can be effectively reduced and the dimension accuracy was nearly equal to the fifth class of cutting gears. Cai et al. [3] proposed the alternative die method for the precision forging of cylindrical gears, and the effects of different tools on forming load and metal flow were studied. A forward extrusion of high-grade aluminium (AA1100) was designed by Tiernan et al. [4], and the influences of reduction ratio, die angle and die land on extrusion force were studied. Michalczyk et al. [5] applied the cold extrusion process to manufacture the internal spine sleeves. The temperature zone distributions of final product were determined. Zuo et al. [6] designed the relief-cavity method for the precision forging of spur gears, and the tooth deviation of forged gears was predicted by numerical simulation and verified by experiments. Kanani, Lalwani [7] focused on the forming load reduction in the cold forging of spur gears with pure aluminium. Their results show that the designed die with relief hole can be used to manufacture gear-like parts, and the force was remarkably reduced. Silveira, Schaeffer [8] investigated the influence of different prestressing levels on the tooth dimension of cold extruded gears by numerical simulation analysis.

Although the forging and extrusion technologies have significant advantages, it is well-known that the dimensional accuracy or surface roughness of forged or extruded gears frequently fails to satisfy the requirement of final parts. With the growing market demand for high-quality gears in the heavy machinery industry, there has been an increased interest in manufacturing gears by the precision forming technologies such as the compound forming process of cold extrusion and precision finishing. Stone et al. [9] developed the cold ironing operation of thick-walled cylinders as the post-process for near-net-shape manufacture. The final dimensions and surface sizing quality of formed parts can be improved. Franulovic et al. [10] studied the influence laws of the pith errors on the forging load of spur gears, and the significant effects of the pitch errors obtained by the experimental analysis were validated. The compound forming process of forging-finishing-extrusion was presented to manufacture conjunction gears by Li et al. [11]. The feasibility of this forming process was verified by the finite element (FE) simulation and experimental results. Behrens, Doege [12] proposed the additional cold sizing strategy to achieve the desired accuracy for cold or hot forged gears. The significant

advantages of this process were confirmed by the numerical and experimental results. Chang et al. [13] proposed a cold ironing operation as the post-forging process for forged gears. Their results revealed that the dimensional errors can be predicted and surface quality can be remarkably improved. Liu et al. [14] simulated the cold sizing operation of spur gear with large module. It was observed that appropriate gear reduction was useful to enhance the tooth dimensional accuracy of forged gears. Li et al. [15] compared the ironing finishing and compressing finishing methods for hot-forged gears on the finishing load, surface roughness and dimensional errors.

At present, the dimensional accuracy of cold extruded sun gear frequently fails to meet the requirement of final parts, which limits the application and promotion of cold extrusion technology in commercial production of the highest quality sun gear. This is primarily due to the sun gear has two kinds of tooth shapes (external gear and internal spline), and the inner metal flow in the forming process is extremely complex, which makes the tooth accuracy difficult to control. Thus, the evolution of tooth deviations is still an important engineering issue in the precision finishing of spur gears. Qin, Balendra [16] established an elastic-plastic model to predict the influences of die-elasticity deformation during the forward extrusion. Ou, Balendra [17] investigated the elastic deflections of the forging dies using numerical simulation and developed a FE strategy to modify the die profiles based on the nominal dimensions of forging dies. A reasonable prediction method was presented by Lee et al. [18] for the machined and shrink-fitted die dimensions in cold forging. Kang et al. [19] introduced a new manufacturing approach for gear forging tools and studied the influences of die elastic deformation in the spur gear forging process. Zuo et al. [20] proposed a theoretical model to predict the profile and lead deviations of spur gears in the hot forging process. Zhuang et al. [21] presented a novel finite element analysis strategy for predicting the tooth deviations during the forging process of spur gears.

Most of the present investigations were focused on manufacturing spur gears with either internal or external teeth. There is a scarcity of research on the dimensional accuracy of sun gear with internal-external tooth shapes. In this study, a

novel precision finishing method with three kinds of spline mandrels was proposed to improve the dimensional accuracy of sun gears formed by the cold extrusion process. Finite element simulations were performed using DEFORM, and a new FE prediction strategy was developed to obtain an in-depth understanding of the deviation distribution laws of the finished sun gear. To confirm the feasibility of the precision finishing method and the reliability of the FE prediction strategy, the experiments of different finishing tools were conducted. Finally, the influences of different finishing tools on tooth deformation, tool stress, forming load and tooth accuracy were examined to determine the optimal reshaping tool for commercial production of sun gears.

2. Precision finishing method

2.1. Cold extrusion process

Sun gear is a kind of typical gear-like part, which is widely used in the truck transmission system. Fig.1 shows the main parameters and geometry of target sun gear in this study. It can be observed that the sun gear has two kinds of tooth shapes, namely external gear and internal spline. The number of external and internal teeth are 23 and 26, respectively. The modules of external and internal gears are 4 and 2, respectively. And, the pressure angles of external and internal teeth are 20° and 30°, respectively.

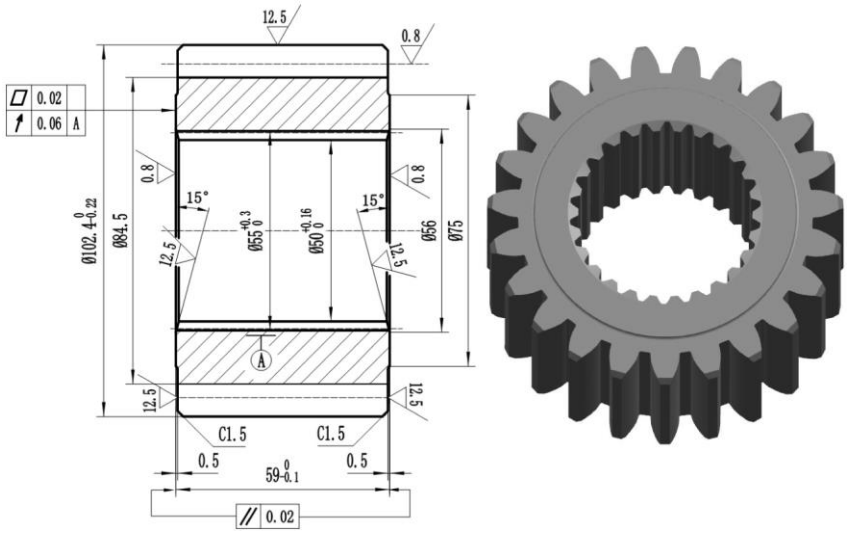

Fig. 1 Main parameters and geometry of sun gear

Fig.2 shows the proposed cold extrusion process of sun gear in the previous investigation. First, a ring-shaped billet, formed by hot-forged, was inserted into the stationary spline mandrel and die. Then, the billet moved downward by the punch, and the internal tooth shapes were gradually formed by the spline mandrel. When the billet was going to pass through the die cavity completely, another billet was placed on the first billet. Then, two billets were pressed by the punch and the internal tooth shapes of the first billet were formed completely, as displayed in Fig. 2(a). Second, the forming principle of external gear was the same as that of the internal spline. The billet with internal spline was put into the toothed die container, then the spline mandrel was passed through the internal tooth by a press and the billet was extruded by the punch so that the external gear was formed, as illustrated in Fig. 2(b).

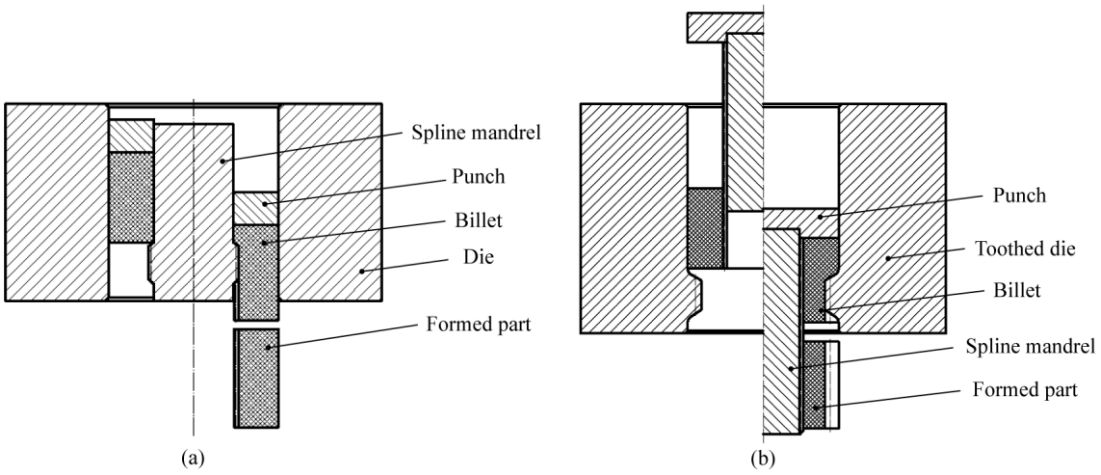

Fig. 2 Cold extrusion process diagrams of sun gear: (a) extruding internal spline; (b) extruding external gear.

The sun gears obtained by the verified experiments of cold extrusion process are shown in Fig. 3, in which the first-formed end of sun gear was defined as the small tooth width, and the big tooth width represents the last formed end. The accuracy of internal-external teeth was inspected using the gear measuring center, as denoted in Fig. 4. The total profile deviation (F_α) and total helix deviation (F_β) are two key indexes of external gear accuracy, and the total M value deviation (F_M) represents the accuracy of internal spline. The inspected results are shown in Fig. 5 and Table 1. The tolerances are for the cutting spur gears and internal spines according to the Chinese Industrial Standard (*CIS*). The M value of internal spline reduced with the increase of tooth width, and the total deviation of M value was 276.4 μm. It can be attributed to the bottom sun gear with small tooth width will have elastic recovery because there is no constraint

from the toothed die. For the accuracy of external gear, with the rise of tooth width, the tooth thickness of external gear decreased firstly, and then grew gradually. Besides, the profile accuracy of external gear was ninth class and lead accuracy was tenth class. The measurement results indicate that the tooth accuracy of extruded sun gear is poor and fails to meet the final product requirements. Therefore, it is necessary to add the precision finishing process to improve the tooth accuracy of the extruded sun gear.

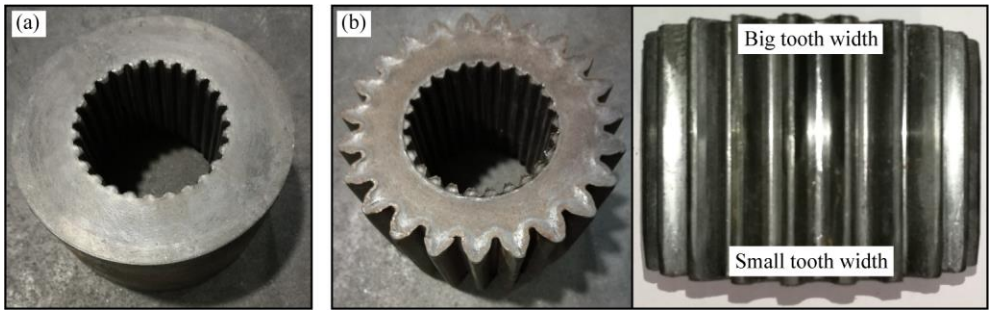

Fig. 3 Pre-formed gears: (a) extruded internal spline; (b) extruded external gear.

Fig. 4 Gear measuring center

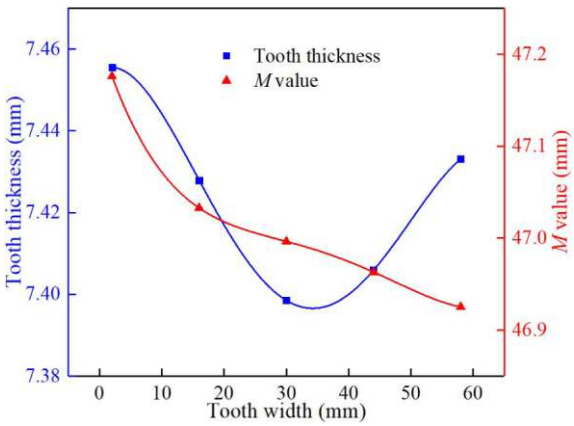

Fig. 5 Tooth thickness and *M* value distributions of extruded sun gear

Table 1 Deviations and tolerances of extruded sun gear

Items	Deviations (Q)	Tolerances (Q in CIS)
F_α (μm)	30.2 (9)	19 (7), 27 (8), 38 (9), 54 (10)
F_β (μm)	55.9 (10)	20 (7), 28 (8), 39 (9), 56 (10)
F_M (μm)	276.4	100

2.2. Precision finishing method design

According to the tooth accuracy requirements of the target sun gear, the precision finishing method was designed to improve the dimensional accuracy of cold extruded sun gears. The principle of the precision finishing method is that the material radial flow is promoted by the reshaping of external gear, resulting in the internal tooth fits the spline mandrel more closely. Thus, the tooth accuracy of internal spline can be significantly improved while the external gear accuracy is enhanced. The error billet was established by measured tooth thickness and M value of cold extruded gears. The external gear will be reshaped 0.2 mm by the entire tooth sizing method, which means that the tip, flank and root will be all finished, as displayed in Fig. 6. While the internal spline will be finished by three kinds of spline mandrels, which are mandrel with gap, mandrel without gap and interference mandrel. As shown in Fig. 7, the tooth profile of spline mandrel without gap is the same as that of the target internal spline; the dimensional profile of mandrel with gap is 0.1 mm smaller than that of the target internal spline so that there is a clearance of 0.1 mm between the spline mandrel and the billet; the tooth profile of interference mandrel is 0.1 mm larger than that of the target internal spline, resulting in the billet can be preferably constrained by the spline mandrel. Fig. 8 shows a diagram of the designed precision finishing process. The spline mandrel will be first passed through the internal tooth by a press, and then the external gear is reshaped during the cold finishing process.

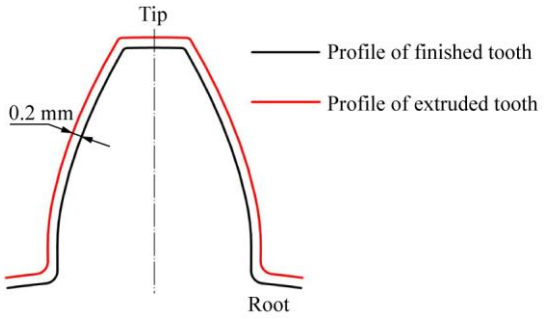

Fig. 6 Schematic diagram of finishing method for external gear

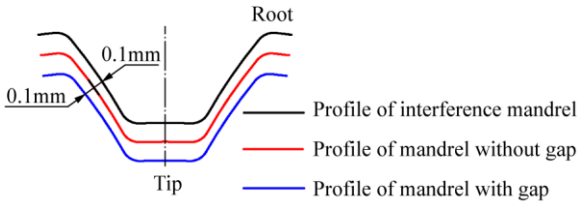

Fig. 7 Schematic diagram of different finishing tools for internal spline

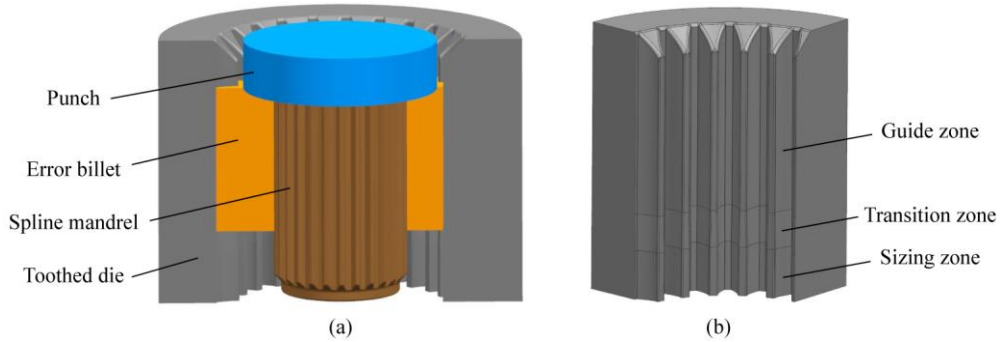

Fig. 8 Schematic of precision finishing process: (a) assemble; (b) toothed die.

3. FE prediction strategy and verified experiment procedure

3.1. Finite element model

The finite element simulation was conducted using the commercial software DEFORM. To focus on the deformation of a complete tooth and save computer processing time, the FE model of precision finishing operation for cold extruded sun gear was performed using a 1/26 section of billet and tools (punch, spline mandrel and toothed die) because of the symmetrical structure, as shown in Fig. 9. The billet was considered as an elastic-plastic body while the tools were defined as rigid bodies because less deformation was observed in the precision finishing process. The billet was divided as tetrahedron mesh and materials around the internal and external teeth were locally refined with the ratio of 0.1. The

friction factor was assumed to be 0.12 and the friction type was shear. The conditions of finite element simulation are summarized in Table 2.

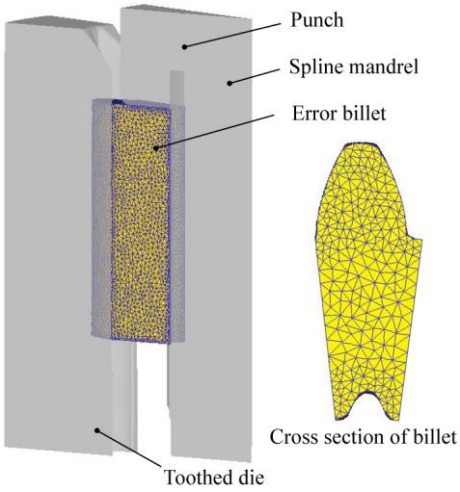

Fig. 9 Finite element model of precision finishing

Table 2 Conditions of precision finishing simulation

Parameters	Values
Punch speed (mm/s)	20
Material of billet	AISI 4120
Mesh number	100000
Mesh size	1
Mesh type	Tetrahedron
Friction factor	0.12
Forming temperature (°C)	20

The billet material is AISI 4120 alloy steel, which is widely used in manufacturing gears because of its good performance in the cold forming process. Table 3 lists the chemical composition of AISI 4120 steel. The true stress-strain curves of billet material at different strain rates are illustrated in Fig. 10.

Table 3 Chemical composition of AISI 4120 (wt. %)

Material	C	Ti	Mn	Cr	Si	Cu	Ni	P	S	Fe
AISI 4120	0.18	0.08	0.90	1.20	0.26	0.22	0.18	0.023	0.02	Balance

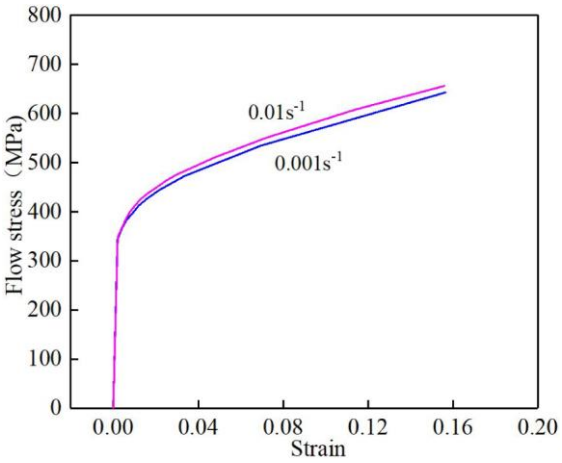

Fig. 10 True stress-strain curve of AISI 4120 at different strain rates

3.2. FE prediction strategy

The present investigations mainly focused on the total errors of spur gears formed by forging or extrusion technology, such as total profile deviation, total helix deviation and cumulative pitch deviation. Due to the target sun gear has two kinds of tooth shapes (external gear and internal spline), and the inner metal flow in the forming process is extremely complex, which makes the tooth accuracy of sun gear difficult to control. To obtain an in-depth understanding of the deviation distribution laws of the finished sun gear, a novel finite element prediction strategy shown in Fig. 11 was developed in this study. First, the simulation results of sun gear formed by the precision finishing method were evenly divided into nine section planes from the lower to the upper ends, thereby obtaining nine tooth profiles. Then, the tooth profiles obtained from numerical simulations were imported into procedure UG to measure the deviations of internal-external teeth. The descriptions of the FE prediction strategy are presented as follows:

(I) The maximum of the single profile deviations (f_α) is assumed to the total profile deviation (F_α), which can be

formulated as:

$$F_{\alpha} = \max\left\{f_{\alpha i}\right\} \qquad \left(i = 1, 2, \cdots, 9\right) \tag{1}$$

where, $f_{\alpha i}$ is the single profile deviation of the i-th section plane.

(II) The differences between the target and finished tooth thickness (left and right surface) are assumed to single helix deviations, and the maximum of the single helix deviations ($f_{\beta L}, f_{\beta R}$) is defined as the total helix deviation (F_{β}), which can be formulated as:

$$f_{\beta Li} = T_{Li} - T_t \qquad \left(i = 1, 2, \cdots, 9\right) \tag{2}$$

$$f_{\beta Ri} = T_{Ri} - T_t \qquad \left(i = 1, 2, \cdots, 9\right) \tag{3}$$

$$F_{\beta} = \max\left\{f_{\beta Li}, f_{\beta Ri}\right\} \qquad \left(i = 1, 2, \cdots, 9\right) \tag{4}$$

where, T_t is half tooth thickness of the target external gear;

T_{Li} is the left tooth thickness of the i-th section plane;

T_{Ri} is the right tooth thickness of the i-th section plane;

$f_{\beta Li}$ is the single helix deviation of left flank of the i-th section plane;

$f_{\beta Ri}$ is the single helix deviation of right flank of the i-th section plane.

(III) The differences of M values between the target and reshaped spline are defined as single M value deviations (f_M), and the maximum of the single M value deviations is assumed to total M value deviation (F_M), which can be formulated as:

$$f_{Mi} = M_t - M_i \qquad \left(i = 1, 2, \cdots, 9\right) \tag{5}$$

$$F_M = \max\left\{f_{Mi}\right\} \qquad \left(i = 1, 2, \cdots, 9\right) \tag{6}$$

where, M_t is the M value of the target internal spline;

M_i is the M value of the i-th section plane;

f_{Mi} is the single M value deviation of the i-th section plane.

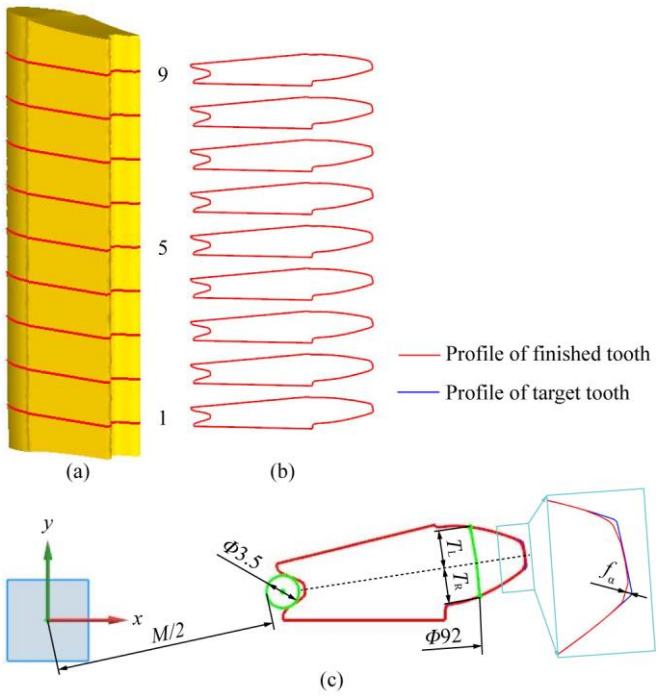

Fig. 11 Novel FE prediction strategy for dimensional deviations of finished sun gear: (a) simulation result; (b) tooth profiles; and (c) measurment method.

3.3. Verified experiment procedure

To verify the feasibility of the precision finishing method and the reliability of the FE prediction strategy, the experiments of different finishing tools were carried out by a hydraulic press with a capacity of 4000 kN. Fig. 12 shows the equipment and tools for the experiments of precision finishing. The materials of tools were AISI D2. To save the experimental cost, the interference mandrel was produced firstly by the wire electrical discharge machine for precision reshaping experiment. When the experiment in interference mandrel was complete, the tooth profile of the spline mandrel was machined by 0.1 mm to obtain the spline mandrel without gap, then the finishing experiment was conducted. Finally, the tooth profile of the mandrel without gap was processed by 0.1 mm to carry out the precision finishing experiment in mandrel with gap. In addition, phosphating and saponification were carried out on the surface of extruded sun gear before precision shaping operation.

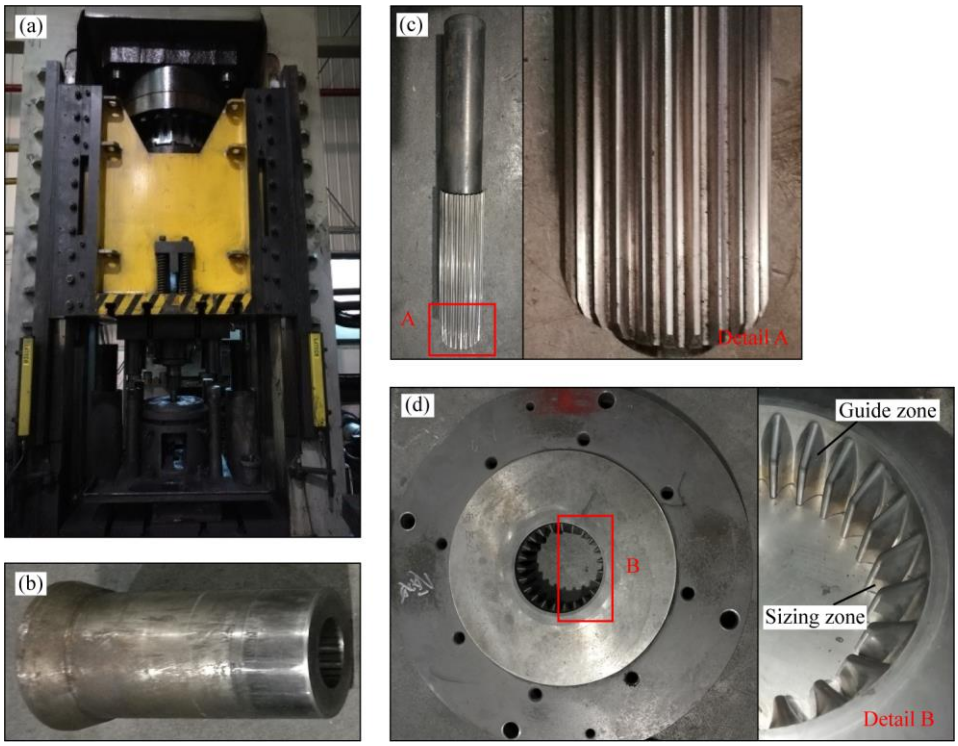

Fig. 12 Experimental equipment and tools: (a) hydraulic press; (b) punch; (c) spline mandrel; and (d) toothed die.

The finished sun gears obtained by different reshaping tools were randomly selected to inspect using the gear measuring center. The total deviations in profile and helix of external gear were inspected for four teeth numbered 1, 5, 10 and 14, which were evenly distributed on the circumference of gears. And, the total *M* value deviation of internal spline was measured for five teeth selected randomly.

4. Results and discussion

4.1. Tooth deformation

Fig. 13 shows the effective stress distributions of the finished sun gear at different finishing tools. When the spline mandrel with gap was applied, due to the gap between the billet and punch, the materials at the upper and lower ends were in an unconstrained state, and the effective stress was the smallest (106 ~ 213 MPa), as illustrated in Fig. 13(a); when the spline mandrel was without gap, it can be seen from Fig. 13(b) that the material effective stress of the upper and lower ends was small (319 ~ 425 MPa) because of the constraint of spline mandrel; when the interference mandrel

was adopted, the billet was well fitted to spline mandrel, thereby the material effective stress of the center layer was uniformly distributed (531 ~ 638 MPa), as denoted in Fig. 13(c).

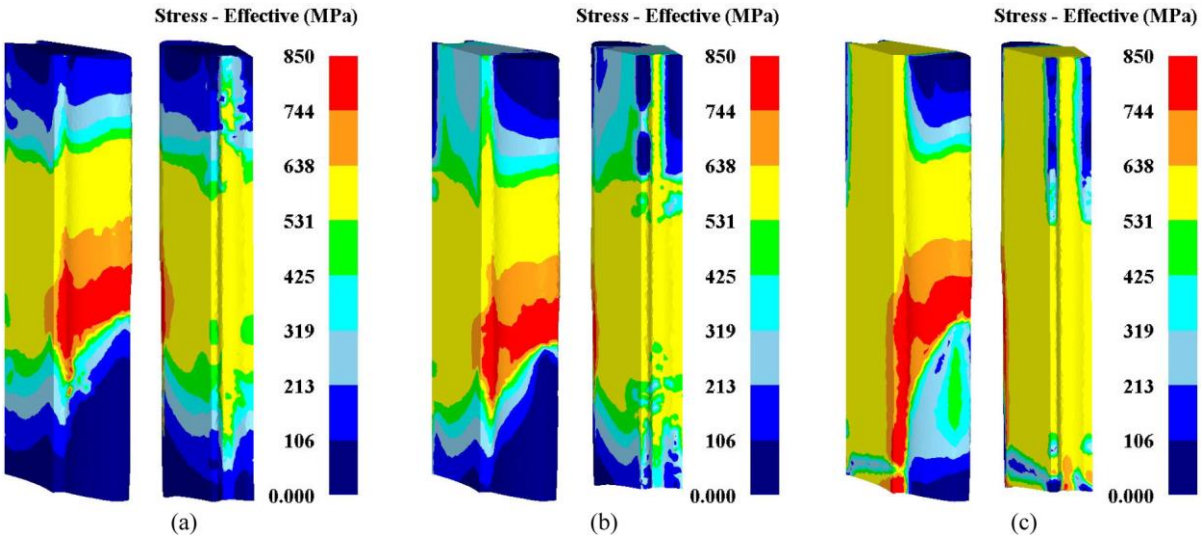

Fig. 13 Effective stress distributions of finished sun gear at different finishing tools: (a) mandrel with gap; (b) mandrel without gap; and (c) interference mandrel.

The effective strain distributions of deformation cross-sections with different reshaping tools are displayed in Fig. 14. It can be concluded that the deformation zone of external gear was the entire tooth surface, but that of internal spline was different because of different spline mandrels for precision finishing operation. When the spline mandrel was with gap, less plastic deformation or even only elastic deformation was observed in the internal spline, as shown in Fig. 14(a); when the spline mandrel without gap was adopted, the billet would be constrained by the spline mandrel, and the deformation zone of inner tooth was mainly concentrated on the tooth tip, as illustrated in Fig. 14(b); when the interference mandrel was applied, the billet fitted closely to spline mandrel, leading to the deformation region of internal spline was the whole tooth surface, as denoted in Fig. 14(c). To sum up, when the interference mandrel is used for the precision finishing process, the deformation zones of the finished sun gear are uniformly distributed and the entire profiles of internal-external teeth will occur plastic deformation, so the finishing effect of interference mandrel is better than the spline mandrel with gap and without gap.

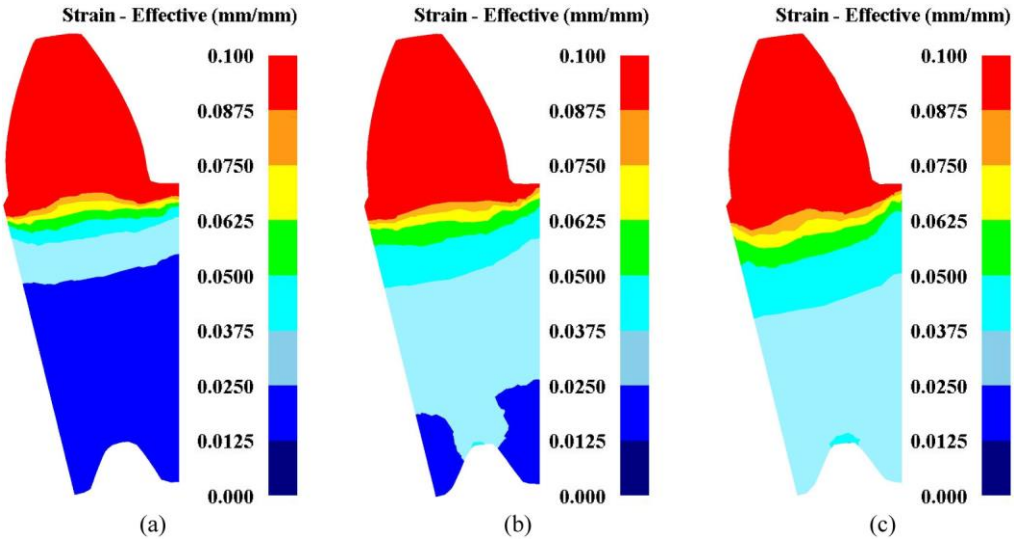

Fig. 14 Effective strain distributions of finished sun gear at different finishing tools: (a) mandrel with gap; (b) mandrel without gap; and (c) interference mandrel.

4.2. Tool stress

In the precision finishing process, the tools (spline mandrel and toothed die) are subjected to considerable stresses exerted by the billet. It is well-known that smaller compressive stress on the tool surfaces means less plastic deformation and longer service life of tools. The max principal stress distributions of spline mandrels illustrated in Fig. 15 are the FE simulation results in different finishing tools, where the negative value is compressive stress and the positive value is tensile stress. It can be seen that the tooth tips of three kinds of spline mandrels are both subjected to large compressive stress during the precision finishing operations, which is the main reason for the plastic deformation of spline mandrels. When the spline mandrel was with gap, due to the clearance between the billet and mandrel, the compressive stress on the mandrel was the smallest, about 300 MPa, as shown in Fig. 15 (a). When the spline mandrel without gap was used, as displayed in Fig. 15 (b), the billet would be constrained by the spline mandrel, the compressive stress of mandrel was primarily in the range of 0~375 MPa and the maximum stress at the tooth tip was 730 MPa. When the interference mandrel was adopted, the maximum compressive stress at the tooth tip of spline mandrel was 1450 MPa because the billet fitted well to mandrel, as denoted in Fig. 15 (c).

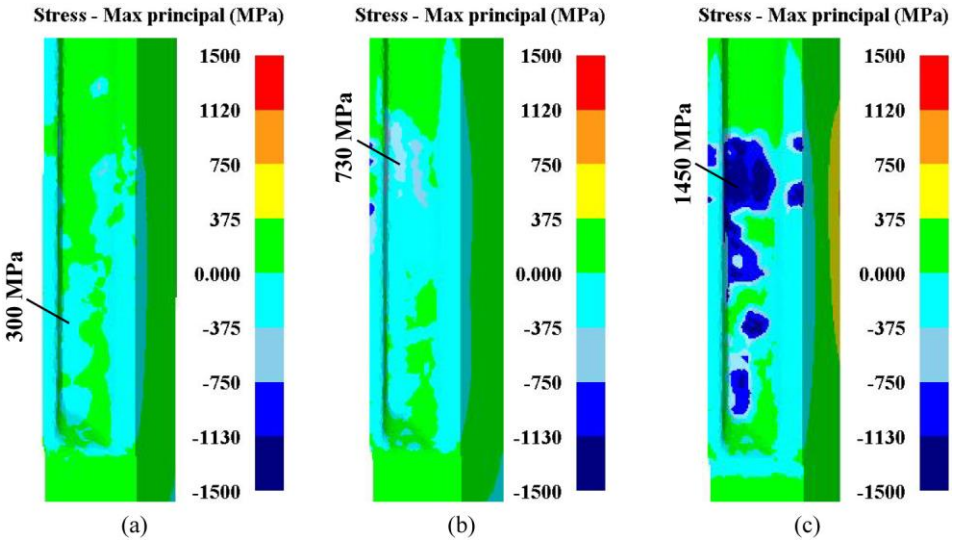

Fig. 15 Max principal stress distributions of different spline mandrels: (a) mandrel with gap; (b) mandrel without gap; and (c) interference mandrel.

Fig. 16 shows the max principal stress distributions of toothed die at different finishing tools. It can be observed that the tip of die tooth was subjected to a tensile stress concentration, as large as 1800 MPa, while the tooth root was under large compressive stress during the precision reshaping operation. When the spline mandrel with gap was applied, as denoted in Fig. 16 (a), the maximum compressive stress occurred at the root, as large as 1350 MPa. When the spline mandrel was without gap, the compressive stress of die surface had the maximum value of 1410 MPa, being 4.3% larger than that of mandrel with gap, as illustrated in Fig. 16 (b). When the interference mandrel was used for the finishing process, the maximum compressive stress of toothed die was 1570 MPa, being 14.0% larger than that of mandrel with gap, as displayed in Fig. 16 (c). Although the maximum compressive stress of the tools with interference mandrel is larger than that of the other two kinds of spline mandrels, the interference mandrel has a better restraint function on the billet, which indicates that this finishing tool can significantly improve the reshaping effect of internal-external gears.

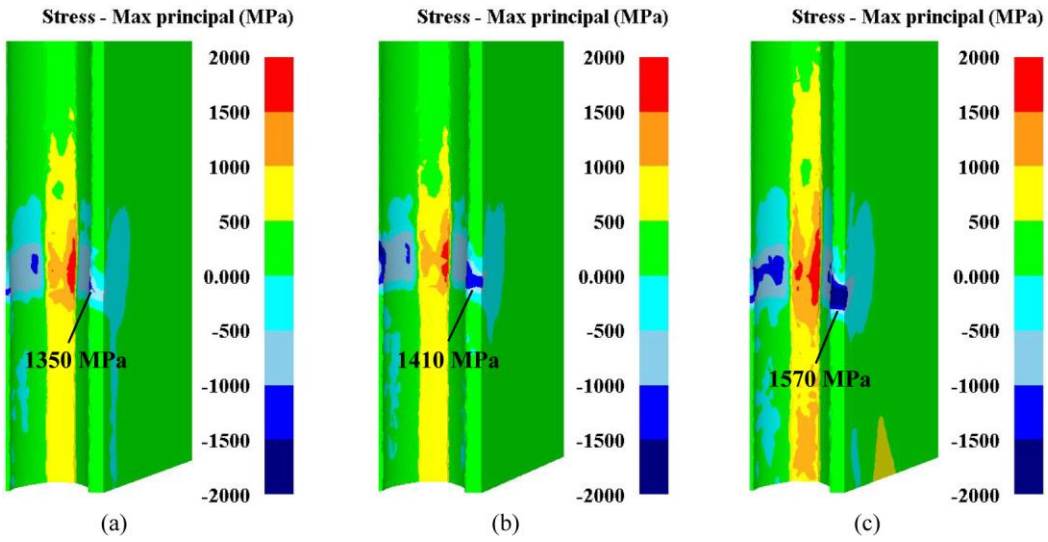

Fig. 16 Max principal stress distributions of toothed die at different finishing tools: (a) mandrel with gap; (b) mandrel without gap; and (c) interference mandrel.

4.3. Forming load

The forming results of the precision finishing process in both FE simulation and experiments are shown in Fig. 17. It can be observed that the surfaces of finished sun gear were smooth, the rounded corners were fully filled, indicating the tooth shapes of internal-external gears are quite sound.

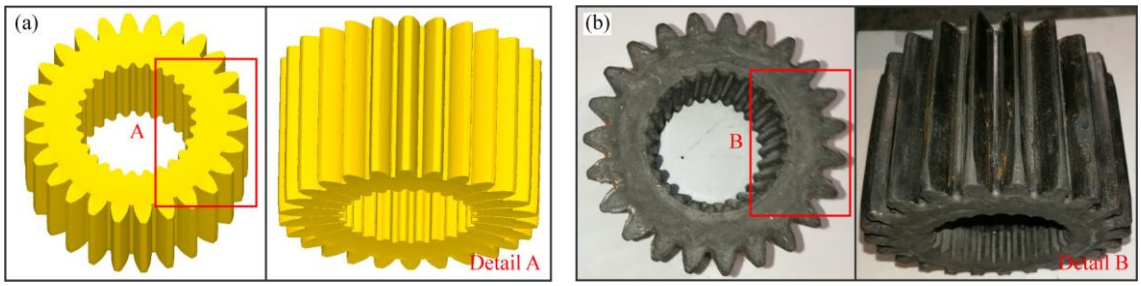

Fig. 17 Results of precision finishing process: (a) FE simulation; and (b) experiment.

Fig. 18 shows the forming load curves of numerical simulations at different finishing tools. With the increase of punch stroke, the billet started to contact with the toothed die under the press of punch, the forming load increased sharply and to a peak value. As the punch stroke continued to rise, partial sun gear had passed through the toothed die, the load gradually reduced to zero. Comparisons of peak loads between FE simulations and confirmed experiments are listed in

Table 4. The peak load in interference mandrel obtained from numerical simulation was 678 kN, being 27.4% and 10.9% larger than that in spline mandrels with gap and without gap, respectively. It can be attributed to the interference mandrel has a better constraint for the billet than mandrels with gap and without gap, so increasing the resistance of material flow in the precision finishing process, leading to the forming load grown. Besides, the experimental results were in good agreement with simulated ones within a maximum error of 7.08%. Therefore, it proves the feasibility of the proposed precision finishing methods and the correctness of simulation results.

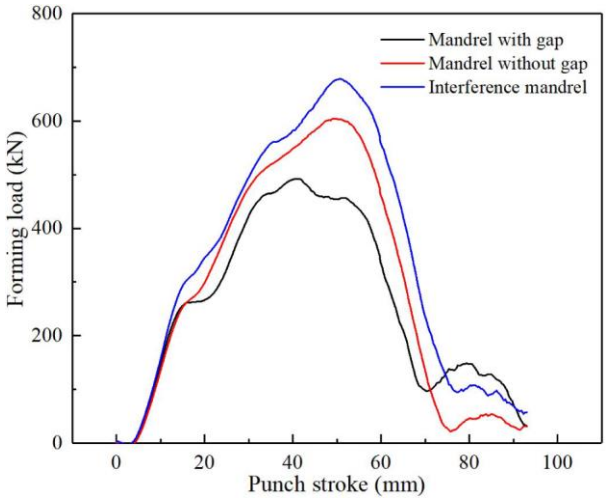

Fig. 18 Forming load curves at different finishing tools

Table 4 Comparison of peak loads between simulations and experiments

Finishing tools	Simulations (kN)	Experiments (kN)	Errors (%)
Mandrel with gap	492	460	6.50
Mandrel without gap	604	570	5.63
Interference mandrel	678	630	7.08

4.4. Tooth accuracy

Fig. 19(a) illustrates the single profile deviation curves of external gear obtained by FE simulations. With the increase of tooth width, the profile deviations first diminished remarkably, then reduced slowly, and finally rose gradually. Moreover, the deviations of finished sun gear obtained by using interference mandrel were smaller than that obtained by

using mandrels both with gap and without gap. This is due to the interference mandrel has a better constraint on the billet, which makes the finishing effect of external gear is preferable.

The total profile deviations of each experimental sun gear formed by different finishing tools are displayed in Fig. 19(b). The total profile deviation obtained using interference mandrel was 0.0172 mm, being 32.8% and 18.5% lower than that using mandrels with gap and without gap, respectively. Besides, it can be observed that the experimental results were larger than the simulated ones. The dimensional differences between the numerical prediction and finished sun gear inspection can be mainly caused by the elastic deformation of tools and thermal deformation of billet, which are not considered in this study.

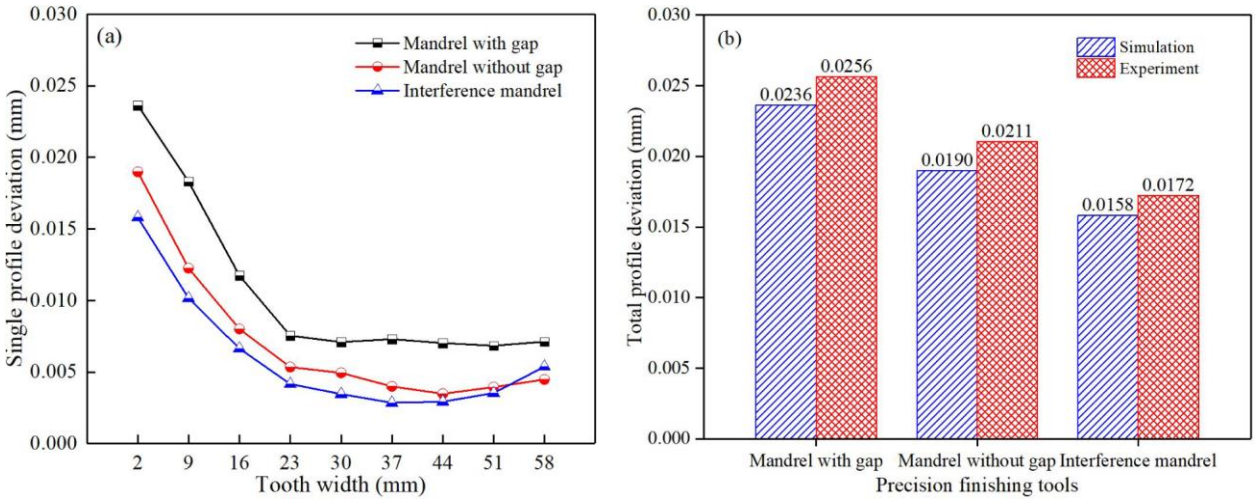

Fig. 19 Profile deviations of external gear at different finishing tools: (a) single profile deviation; (b) total profile deviation.

The helix deviations of external gear obtained by numerical simulations and experiments are shown in Fig. 20. When the mandrel was with gap, the single helix deviations of left and right surfaces reduced significantly with the increase of tooth width, and the maximum value appeared at the lower end of sun gear, as large as 0.0285 mm. When the spline mandrel without gap was adopted, as rising tooth width, the deviations diminished significantly at first, then kept stable and finally increased gradually. Moreover, the total helix deviations obtained from simulation and experiment were

0.0229 and 0.0241 mm, respectively. When the interference mandrel was applied, as increasing tooth width, the single helix errors decreased gradually, and then rose remarkably. Also, the total helix deviation observed at the lower end of reshaped sun gear was 0.0182 mm, being 36.1% and 20.5% lower than that using mandrels with gap and without gap, respectively. It can likewise be seen that the total helix deviations obtained by experiments were larger than of obtained by numerical simulations due to thermal expansion of billet and elastic deformation of finishing tools.

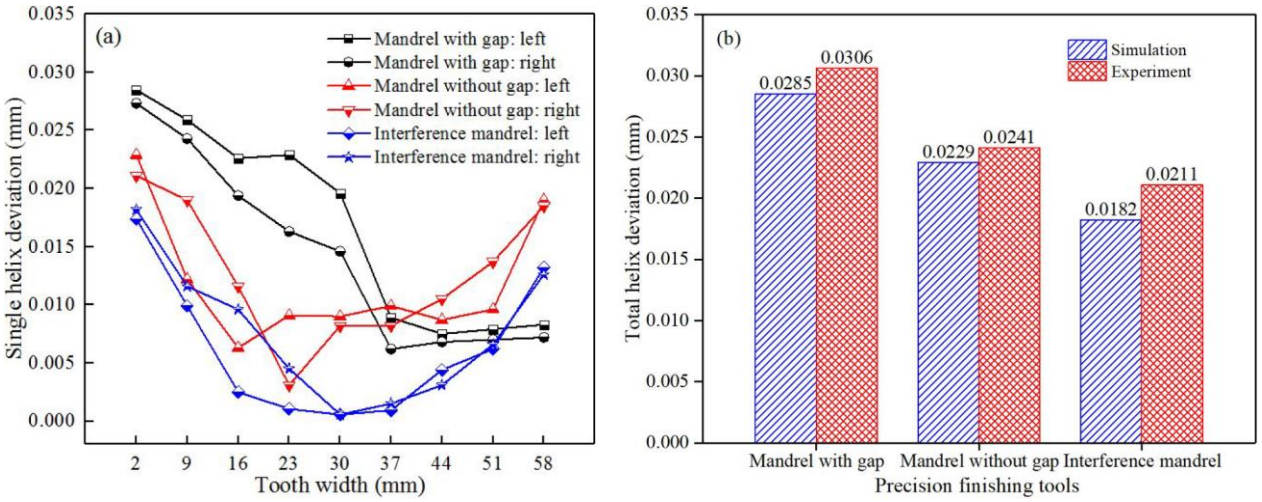

Fig. 20 Helix deviations of external gear at different finishing tools: (a) single helix deviation; (b) total helix deviation.

The *M* value deviations of internal spline shown in Fig. 21 were obtained from both FE simulations and verified experiments. With the increase of tooth width, single *M* value deviation in mandrel with gap grown firstly and then decreased remarkably, and the largest value occurred on the middle region of formed gear, as large as 0.5635 mm. It can be explained that during the process of precision finishing, due to the clearance between the billet and spline mandrel, materials will flow to the inner layer under the push of external gear's reshaping, leading to the tiny upsetting phenomenon of big in the middle region and small at both ends. The single *M* value deviations obtained using mandrel without gap and interference mandrel reduced gradually with increasing tooth width, and the experimental results of total *M* value deviations were 0.1505 and 0.0723 mm, respectively. This finding shows that the constraint effect of spline mandrel can effectively ensure the reshaping quality of internal spline, which is consistent with the above analysis of tools.

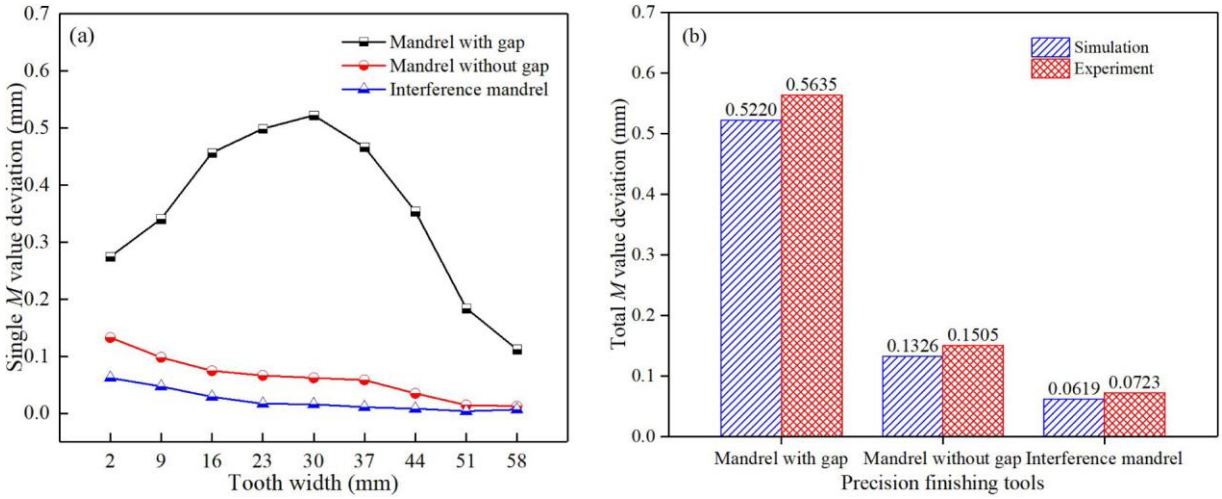

Fig. 21 *M* value deviations of internal spline at different finishing tools: (a) single *M* value deviation; (b) total *M* value deviation.

From the above analysis, it can be concluded that compared with the spline mandrels both with gap and without gap, the interference mandrel has a considerable reshaping effect for internal-external teeth due to the constraint function on the billet. Table 5 provides a comparison of total deviations before and after finishing using interference mandrel. The total deviations in profile, helix and *M* value after reshaping are significantly lower than those before finishing. The profile accuracy of external gear can be improved from ninth to seventh class, tooth lead accuracy can be enhanced from tenth to eighth class, and total *M* value deviation of internal spline is reduced to 72.3 μm, which satisfied the final product requirements. Therefore, it can be considered that the precision finishing method with interference mandrel is effective and recommended to improve the tooth accuracy of cold extruded sun gear.

Table 5 Comparison of total deviations before and after finishing

Before finishing	Profile deviation 5 mm 2:1 20 μm 500:1	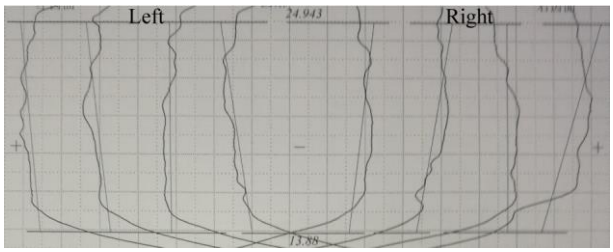
	F_α (Q)	30.2 μm (9)

	Helix deviation 10 mm 1:1 20 μm 500:1	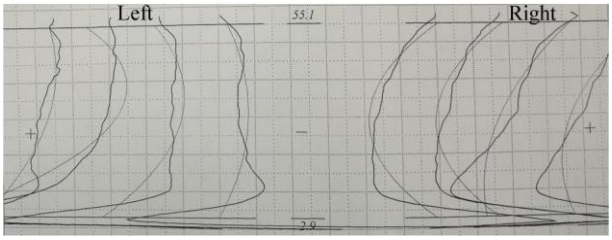
	F_β (Q)	55.9 μm (10)
	F_M	276.4 μm
After finishing	Profile deviation 5 mm 2:1 20 μm 500:1	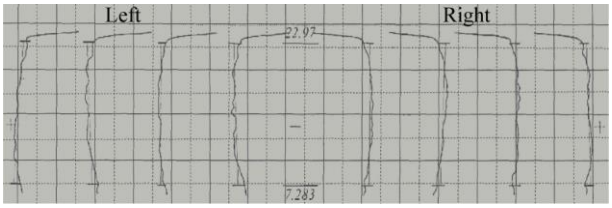
	F_α (Q)	17.2 μm (7)
	Helix deviation 10 mm 1:1 20 μm 500:1	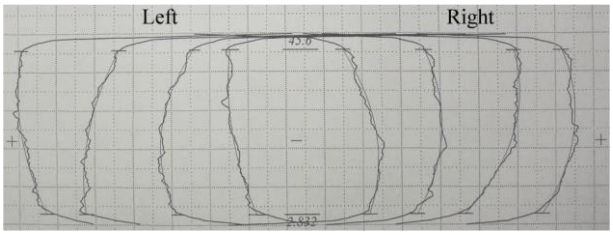
	F_β (Q)	21.1 μm (8)
	F_M	72.3 μm

5. Conclusions

Due to the complex metal flow in the cold extrusion of sun gear, the tooth accuracy of formed sun gear is poor. A novel precision finishing method with three kinds of spline mandrels was proposed in this study to improve the dimensional accuracy of sun gears formed by cold extrusion process, and a new FE prediction strategy was developed to obtain an in-depth understanding of the deviation distribution laws of the finished sun gear. The influences of different finishing tools on tooth deformation, tool stress, forming load and tooth accuracy were examined to determine the optimal

reshaping tool for commercial production of sun gears. The following conclusions can be drawn based on this study:

(1) When the interference mandrel is used for the precision finishing process, the entire profiles of internal-external teeth will occur plastic deformation, and the finishing effect is better than mandrels both with gap and without gap. Therefore, the interference mandrel is recommended as the optimal reshaping tool to improve the tooth accuracy of cold extruded sun gear.

(2) Although the maximum compressive stress of the tools with interference mandrel is larger than mandrels both with gap and without gap, the interference mandrel has a better restraint function on the billet, which indicates that this finishing tool can significantly improve the reshaping effect of internal-external gears.

(3) The results of both simulations and experiments show that the tooth shapes of reshaped sun gear are quite sound, and the peak loads obtained by experiments are in good agreement with simulated ones within a maximum error of 7.08%, which proves the feasibility of the proposed precision finishing methods and the correctness of simulation results.

(4) The profile accuracy of external gear can be improved from ninth to seventh class, tooth lead accuracy is enhanced from tenth to eighth class, and total M value deviation of internal spline can be reduced to 72.3 μm, demonstrating the accuracy of extruded sun gear is effectively enhanced. The simulation results of teeth deviations are well agreed with the experimental results, which verifies the reliability of the FE prediction strategy.

Declarations

Ethical Approval Not applicable

Consent to Participate Not applicable

Consent to Publish All authors agree to publication in The International Journal of Advanced Manufacturing Technology.

Authors Contributions Zuofa Liu and Wenjie Feng conceived and designed the study. Zuofa Liu, Xi Wang, and Jie Zhou performed the experiments. Jie Zhou provided funding. Zuofa Liu and Jie Zhou wrote the paper. Wenjie Feng,

Qiang Liang, Zhiyuan Qu and Xi Wang reviewed and edited the manuscript. All authors read and approved the manuscript.

Funding This research was financially supported by the National Key Research and Development Program of China (No.2018YFB1106504) and Postdoctoral Science Foundation of Chongqing Natural Science Foundation (No. cstc2020jcyj-bshX0006).

Competing Interests The authors declare that they have no conflict of interest.

Availability of data and materials All data, models, and code generated or used during the study appear in the submitted article.

References

1. Song J-H, Im Y-T (2007) The applicability of process design system for forward extrusion of spur gears. Journal of Materials Processing Technology 184 (1-3):411-419. doi:10.1016/j.jmatprotec.2006.12.009
2. Choia JC, Choi Y (1999) Precision forging of spur gears with inside relief. International Journal of Machine Tools and Manufacture 39 (10):1575-1588. doi:10.1016/S0890-6955(99)00015-2
3. Cai J, Dean TA, Hu ZM (2004) Alternative die designs in net-shape forging of gears. Journal of Materials Processing Technology 150 (1-2):48-55. doi:10.1016/j.jmatprotec.2004.01.019
4. Tiernan P, Hillery MT, Draganescu B, Gheorghe M (2005) Modelling of cold extrusion with experimental verification. Journal of Materials Processing Technology 168 (2):360-366. doi:10.1016/j.jmatprotec.2005.02.249
5. Michalczyk J, Wiewiórowska S, Muskalski Z (2018) The development and modeling of an innovative process of forming the internal toothing of flange coupling spline sleeves. Archives of Metallurgy and Materials 63 (4):1981-1986. doi:10.24425/amm.2018.125133
6. Zuo B, Wang B-y, Li Z, Zheng M-n, Zhu X-x (2015) Design of relief-cavity in closed-precision forging of gears. Journal of Central South University 22 (4):1287-1297. doi:10.1007/s11771-015-2645-0
7. Kanani JB, Lalwani DI (2020) An experimental and FEA investigation of near-net-shape cold forging of spur gear.

Materials Today: Proceedings. doi:10.1016/j.matpr.2020.07.422

8. Silveira FD, Schaeffer L (2018) Evaluation of different levels of prestressing for cold forging tools by numerical simulation analysis. The International Journal of Advanced Manufacturing Technology 98 (9-12):2487-2495. doi:10.1007/s00170-018-2351-9

9. Stone ERH, Cai J, Hu ZM, Dean TA (2003) An exercise in cold ironing as the post-forging operation for net-shape manufacture. Journal of Materials Processing Technology 135 (2-3):278-283. doi:10.1016/s0924-0136(02)00858-0

10. Franulovic M, Markovic K, Vrcan Z, Soban M (2017) Experimental and analytical investigation of the influence of pitch deviations on the loading capacity of HCR spur gears. Mechanism and Machine Theory 117:96-113. doi:10.1016/j.mechmachtheory.2017.07.006

11. Li S, Ji H, Wang B, Mu Y (2019) Numerical analysis and experimental validation of conjunction gear via hot forging-upsetting finishing-radial extrusion. Archives of Civil and Mechanical Engineering 19 (2):391-404. doi:10.1016/j.acme.2018.11.006

12. Behrens BA, Doege E (2004) Cold Sizing of Cold- and Hot-Formed Gears. CIRP Annals 53 (1):239-242. doi:10.1016/s0007-8506(07)60688-x

13. Chang YC, Hu ZM, Kang BS, Dean TA (2002) A study of cold ironing as a post-process for net-shape manufacture. International Journal of Machine Tools and Manufacture 42 (8):945-952. doi:10.1016/S0890-6955(02)00022-6

14. Liu GH, Zhong ZP, Bian Y, Li Q (2012) Numerical Simulation on Precision Forging Process for Spur-Gear with Large Module. Advanced Materials Research 538-541:927-931. doi:10.4028/www.scientific.net/AMR.538-541.927

15. Li Z, Wang B, Ma W, Yang L (2016) Comparison of ironing finishing and compressing finishing as post-forging for net-shape manufacturing. The International Journal of Advanced Manufacturing Technology 86 (9-12):3333-3343. doi:10.1007/s00170-016-8424-8

16. Qin Y, Balendra R (1997) FE simulation of the influence of die-elasticity on component dimensions in forward

extrusion. International Journal of Machine Tools & Manufacture 37 (2):183-192. doi:10.1016/0890-6955(95)00102-6

17. Ou H, Balendra R (1998) Die-elasticity for precision forging of aerofoil sections using finite element simulation. Journal of Materials Processing Technology 76 (1-3):56-61. doi:10.1016/S0924-0136(97)00315-4
18. Lee Y, Lee J, Kwon Y, Ishikawa T (2004) Modeling approach to estimate the elastic characteristics of workpiece and shrink-fitted die for cold forging. Journal of Materials Processing Technology 147 (1):102-110. doi:10.1016/j.jmatprotec.2003.12.008
19. Kang JH, Lee KO, Je JS, Kang SS (2007) Spur gear forging tool manufacturing method considering elastic deformation due to shrink fitting. Journal of Materials Processing Technology 187-188:14-18. doi:10.1016/j.jmatprotec.2006.11.161
20. Zuo B, Wang B, Li Z, Li N, Lin J (2016) An investigation of involute and lead deflection in hot precision forging of gears. The International Journal of Advanced Manufacturing Technology 88 (9-12):3017-3030. doi:10.1007/s00170-016-9003-8
21. Zhuang W, Han X, Hua L, Xu M, Chen M (2019) FE prediction method for tooth variation in hot forging of spur bevel gears. Journal of Manufacturing Processes 38:244-255. doi:10.1016/j.jmapro.2019.01.022

Figures

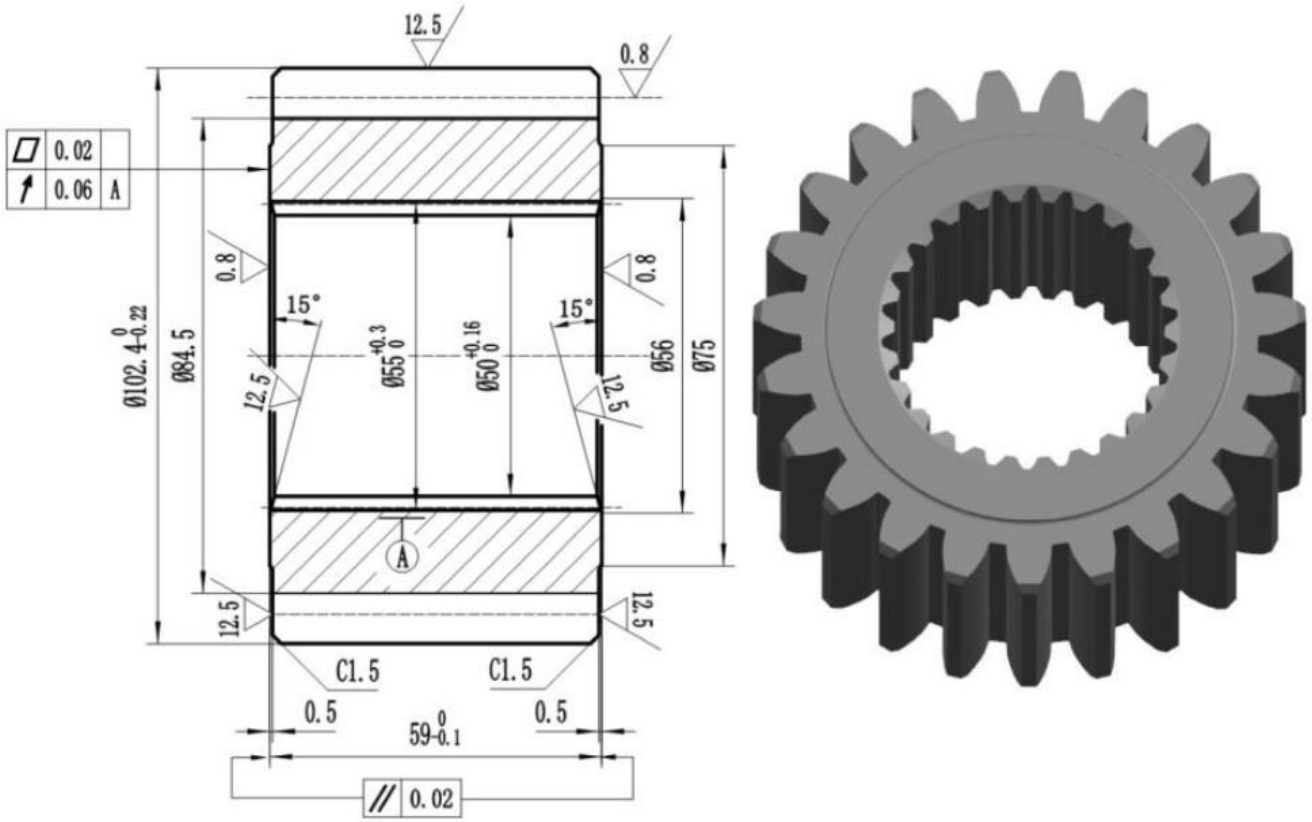

Figure 1

Main parameters and geometry of sun gear

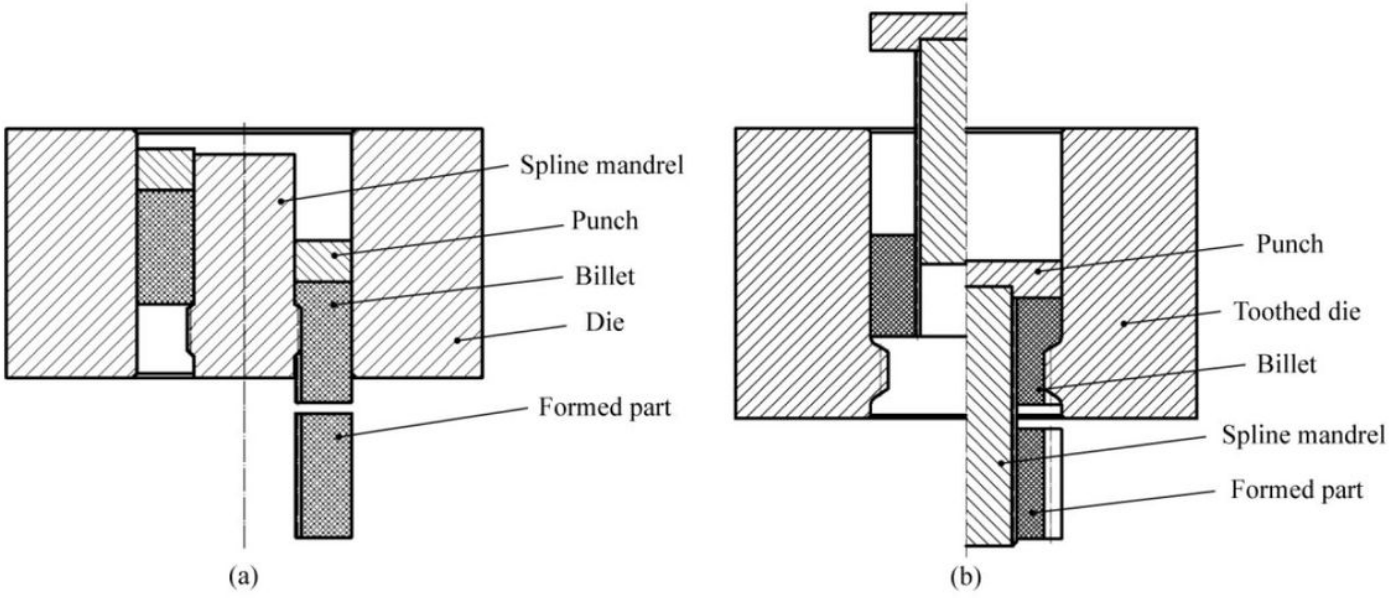

Figure 2

Cold extrusion process diagrams of sun gear: (a) extruding internal spline; (b) extruding external gear

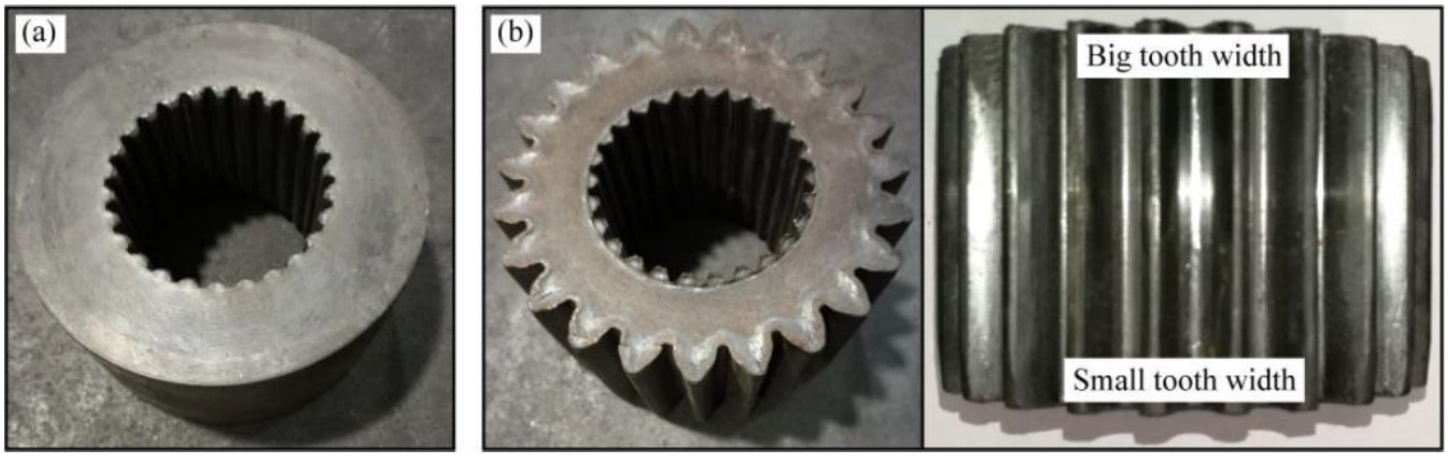

Figure 3

Pre formed gears: (a) extruded internal spline; (b) extruded external gear.

Figure 4

Gear measuring center

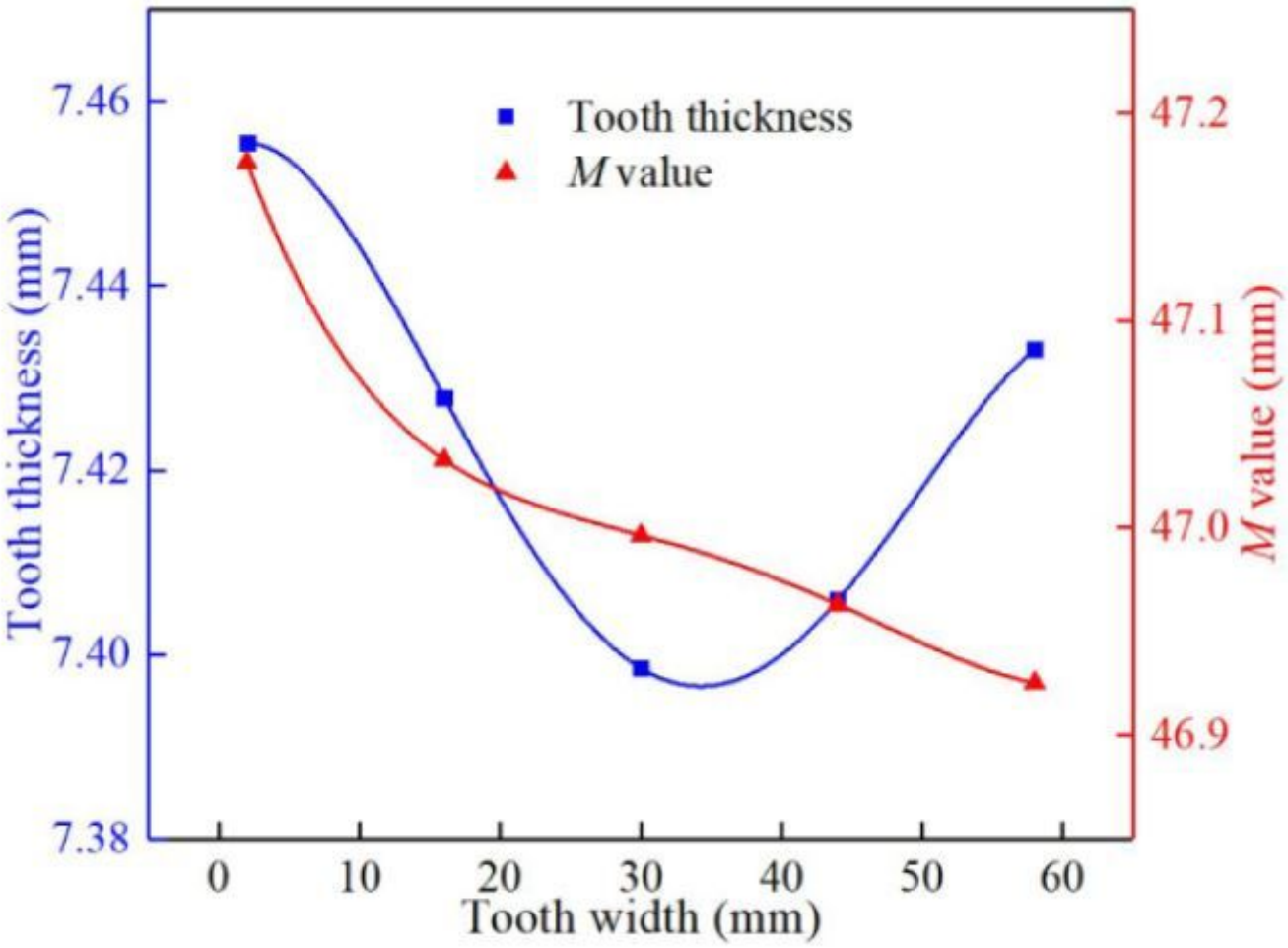

Figure 5

Tooth thickness and M value distributions of extruded sun gear

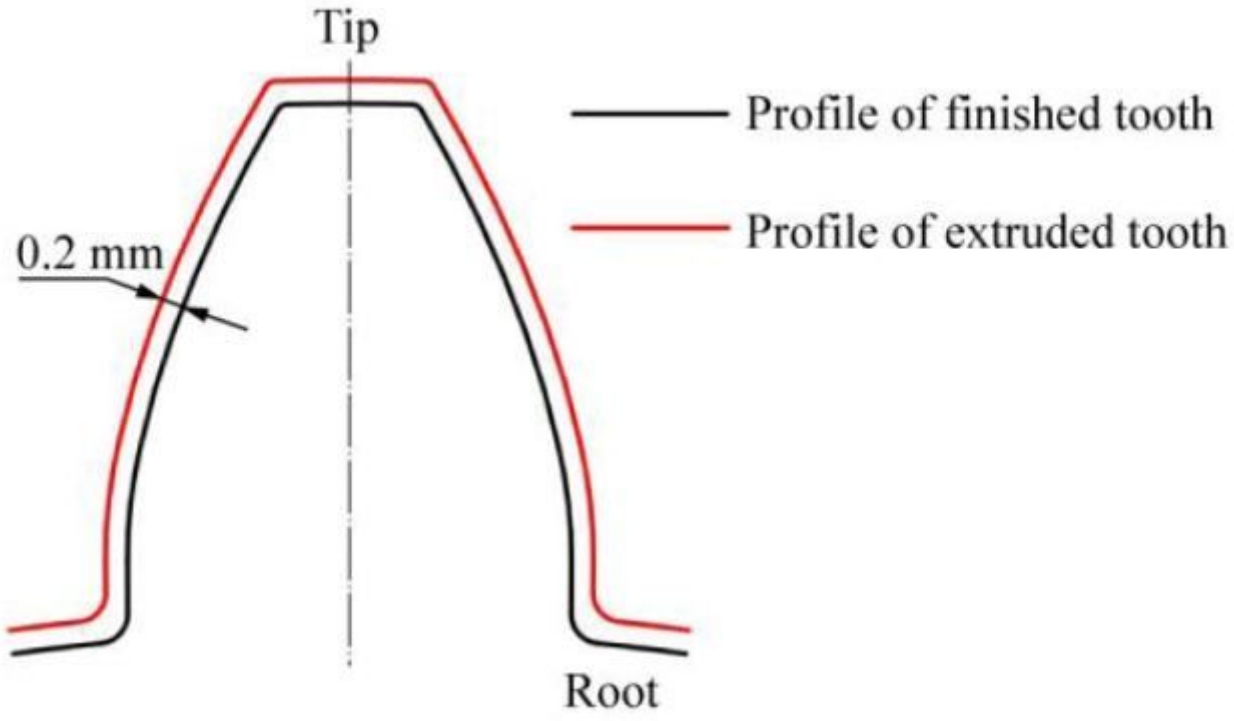

Figure 6

Schematic diagram of finishing method for external gear

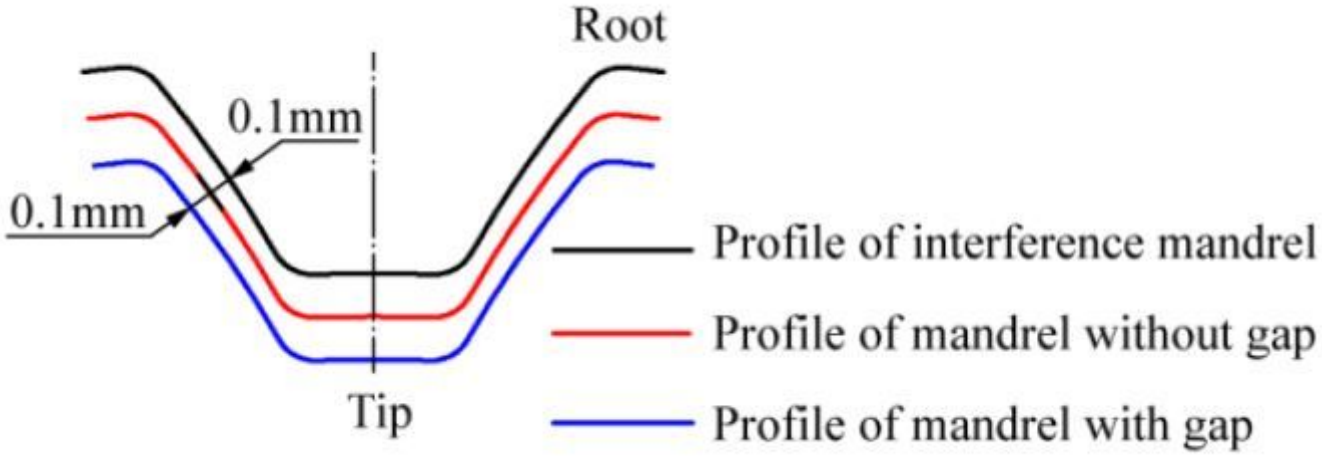

Figure 7

Schematic diagram of different finishing tools for internal spline

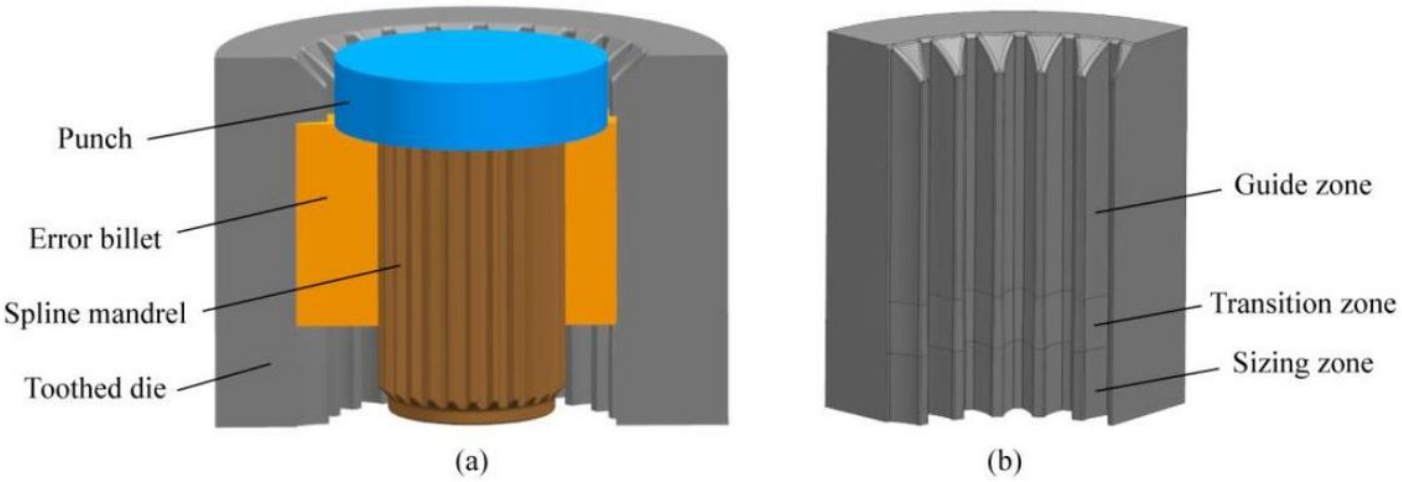

Figure 8

Schematic of precision finishing process: (a) assemble; (b) toothed die.

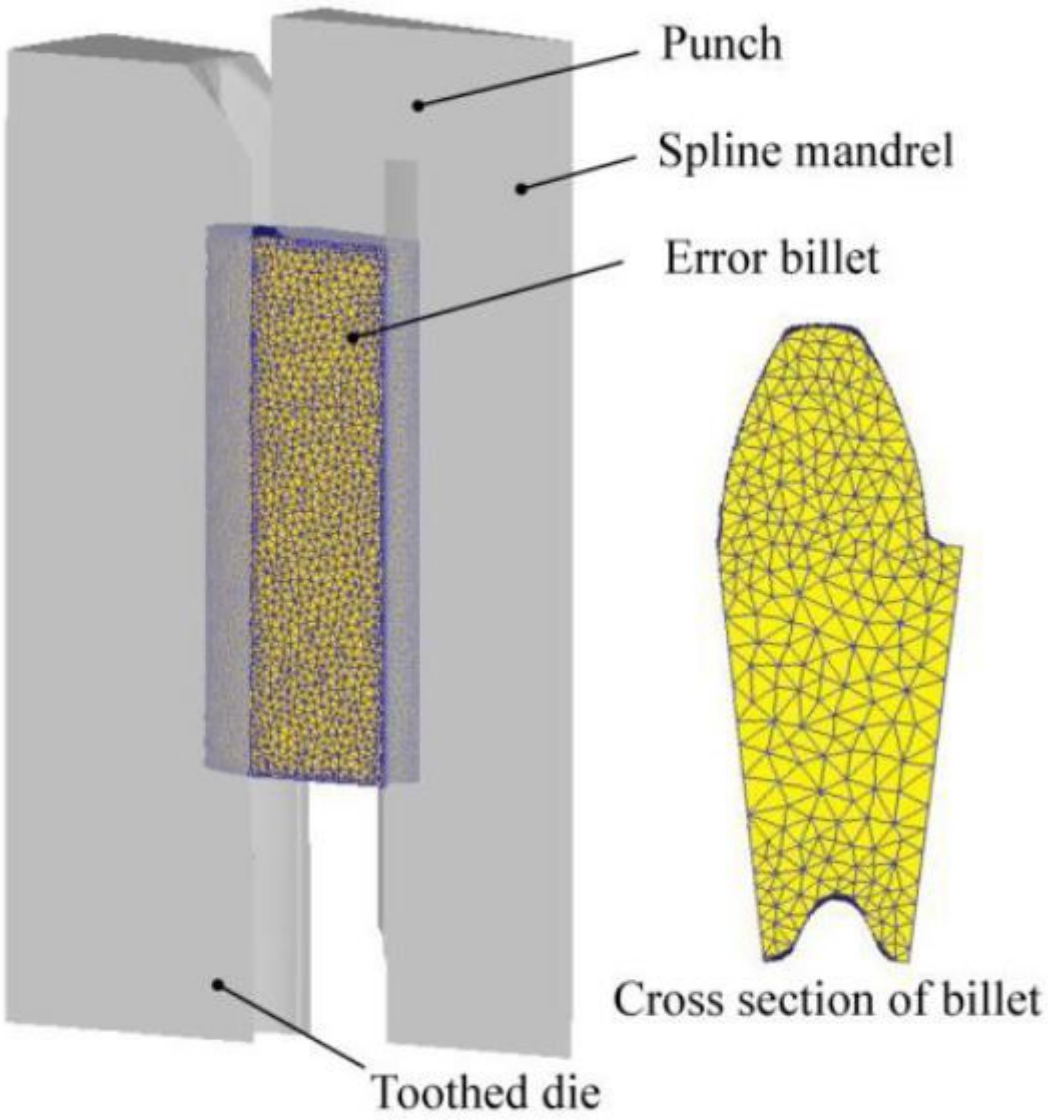

Figure 9

Finite element model of precision finishing

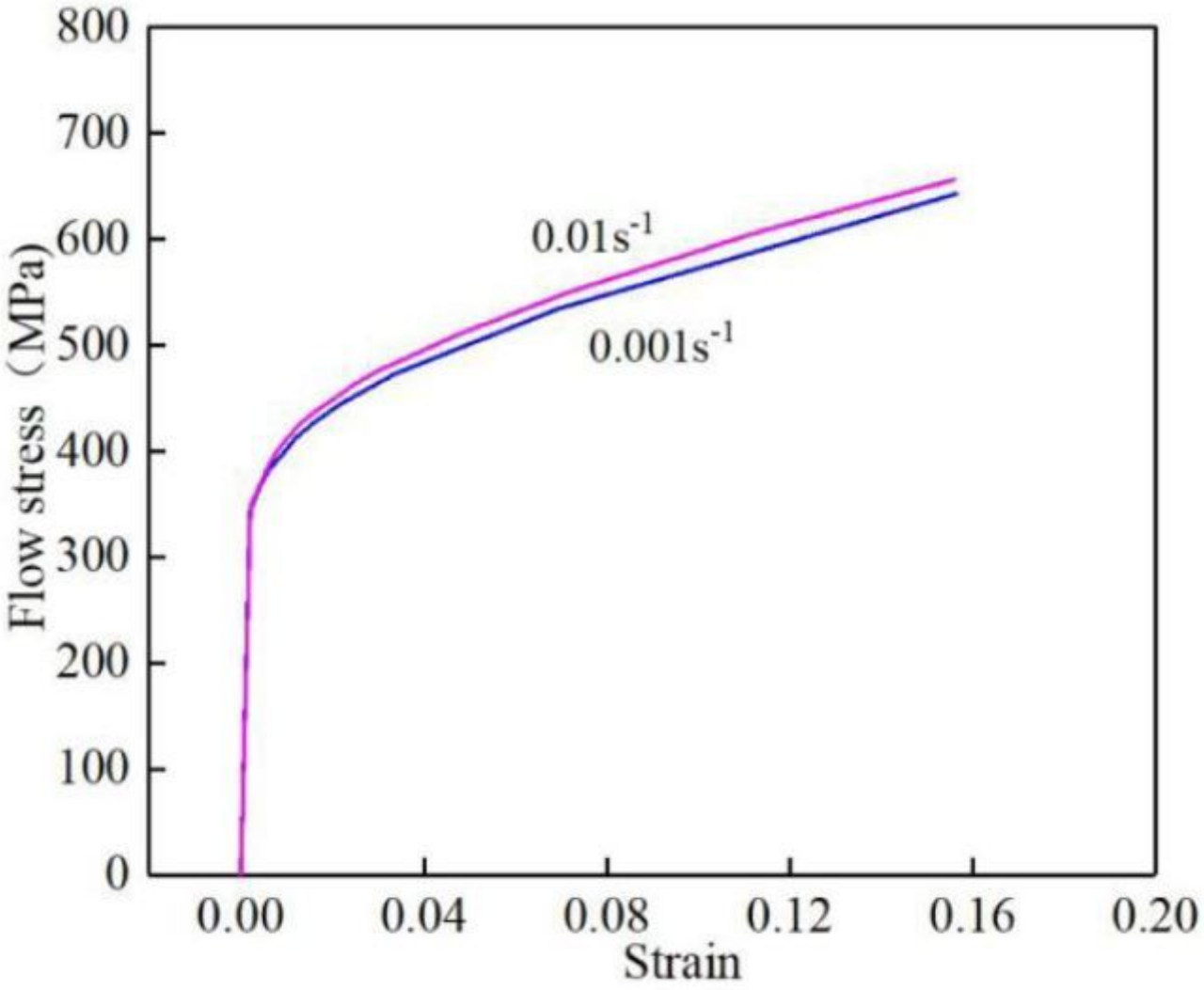

Figure 10

True stress strain curve of AISI 4120 at different strain rates

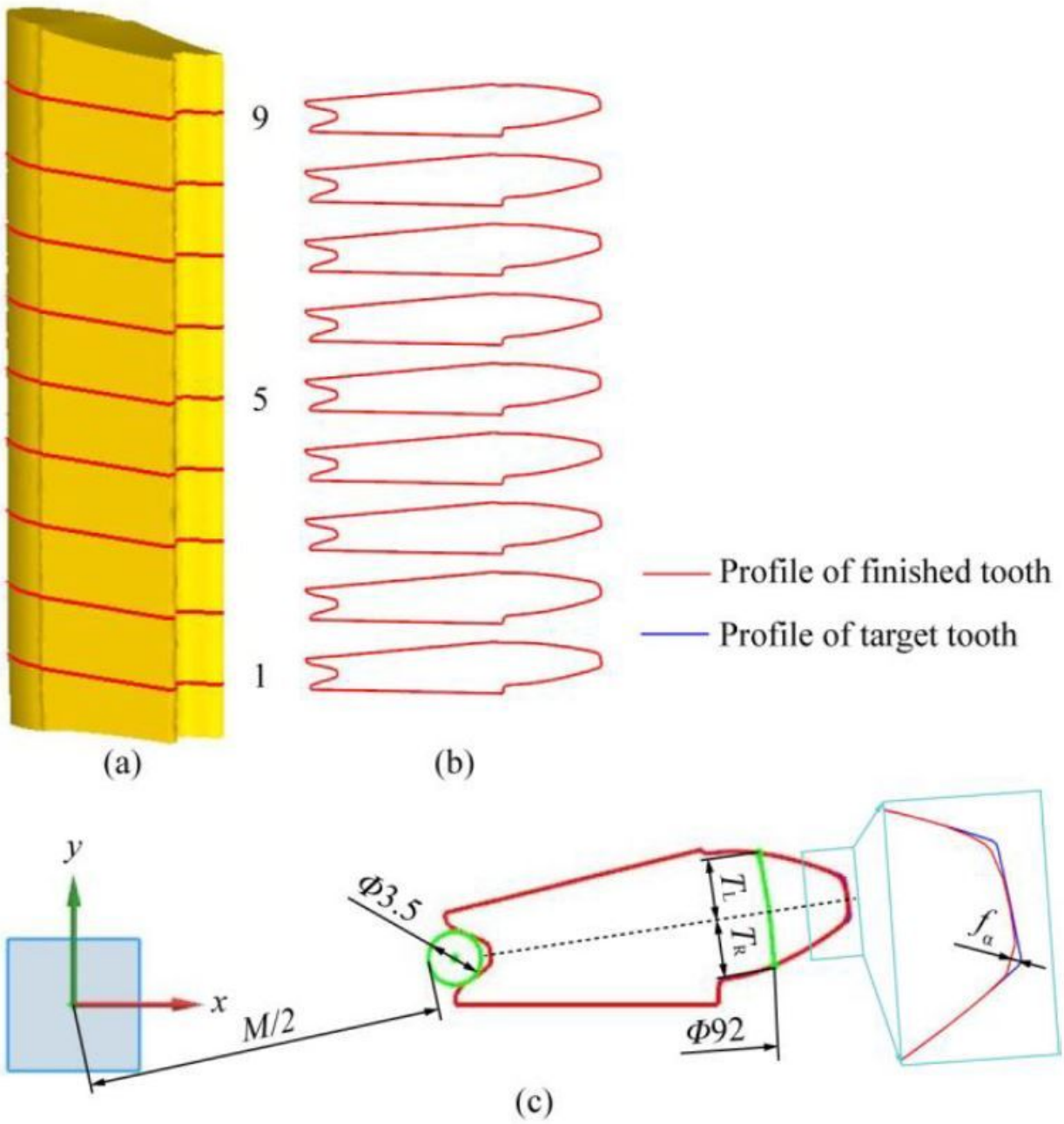

Figure 11

Novel FE prediction strategy for dimensional deviations of finished sun gear: (a) simulation result; (b) tooth profiles; and (c) measurment method.

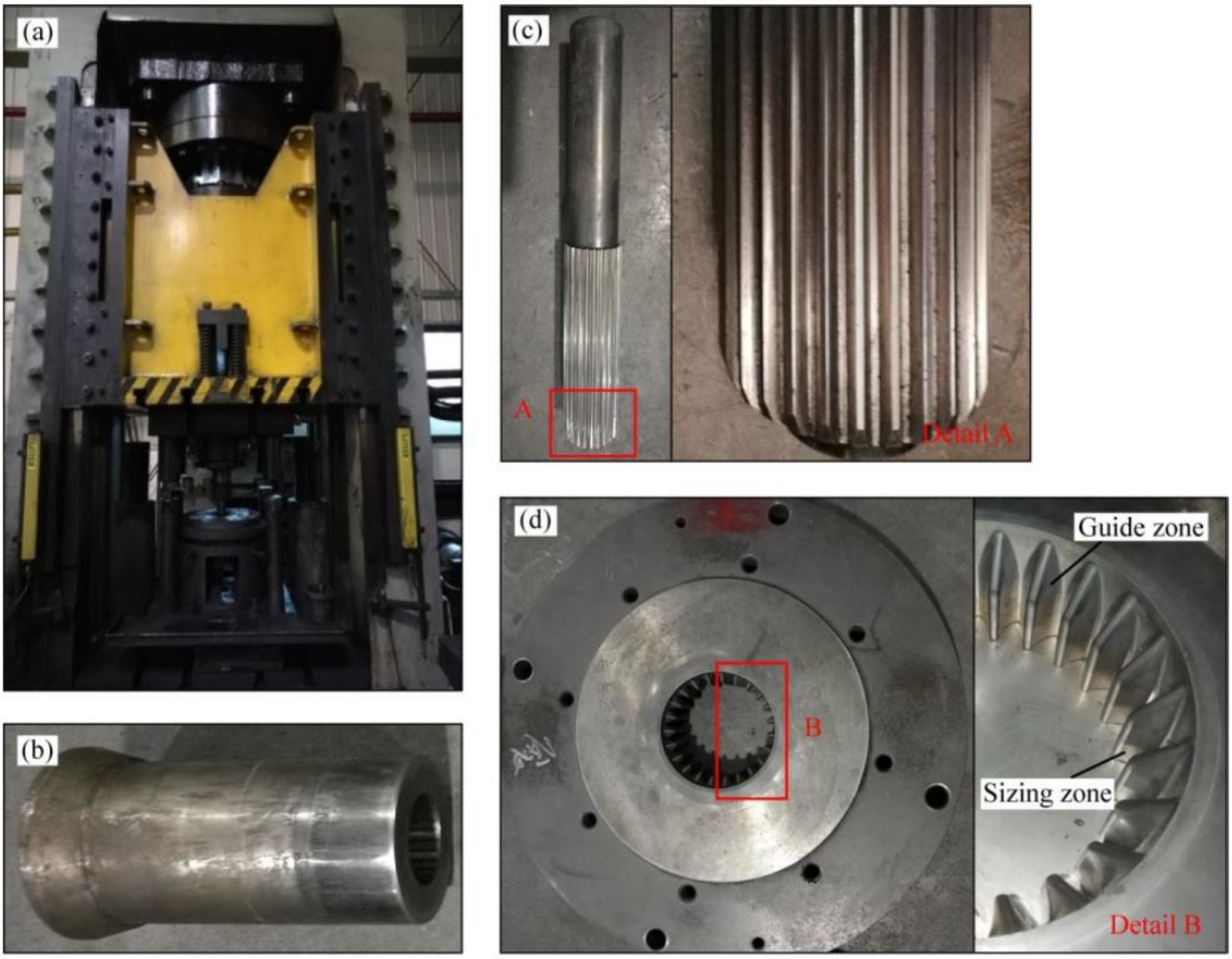

Figure 12

Experimental equipment and tools: (a) hydraulic press; (b) punch; (c) spline mandrel; and (d) toothed die.

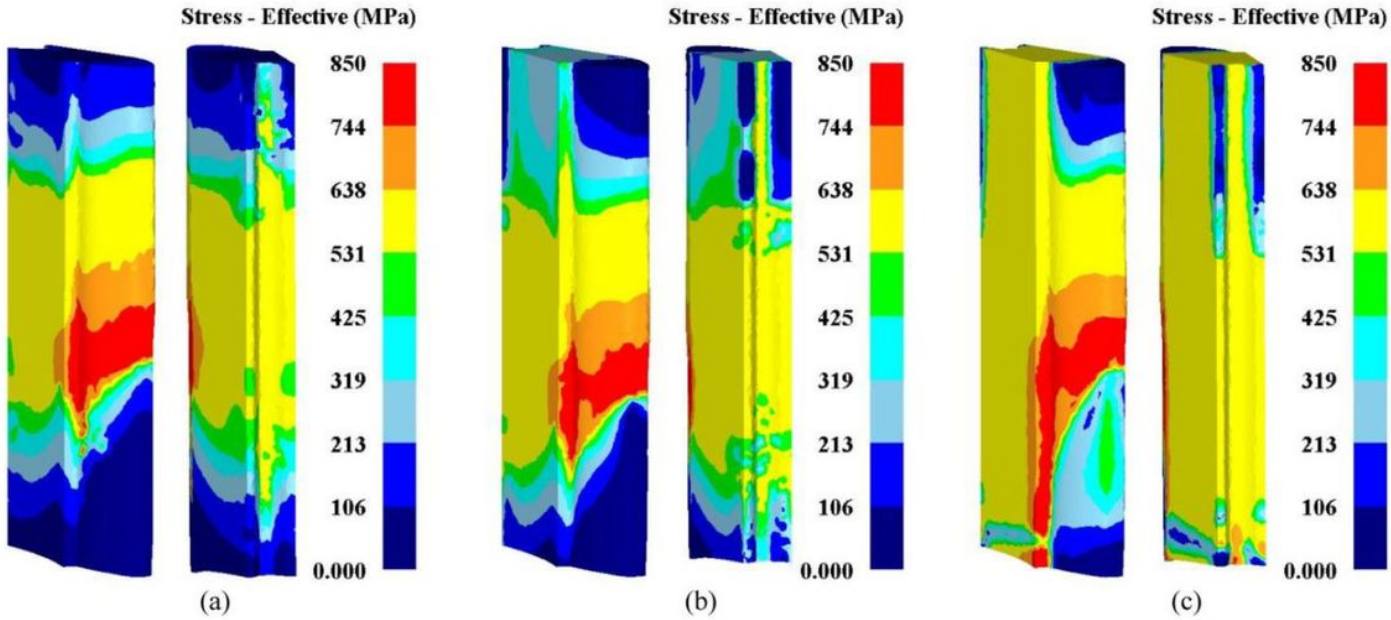

Figure 13

Effective stress distributions of finished sun gear at different finishing tools: (a) mandrel with gap; (b) mandrel without gap; and (c) interference ma ndrel.

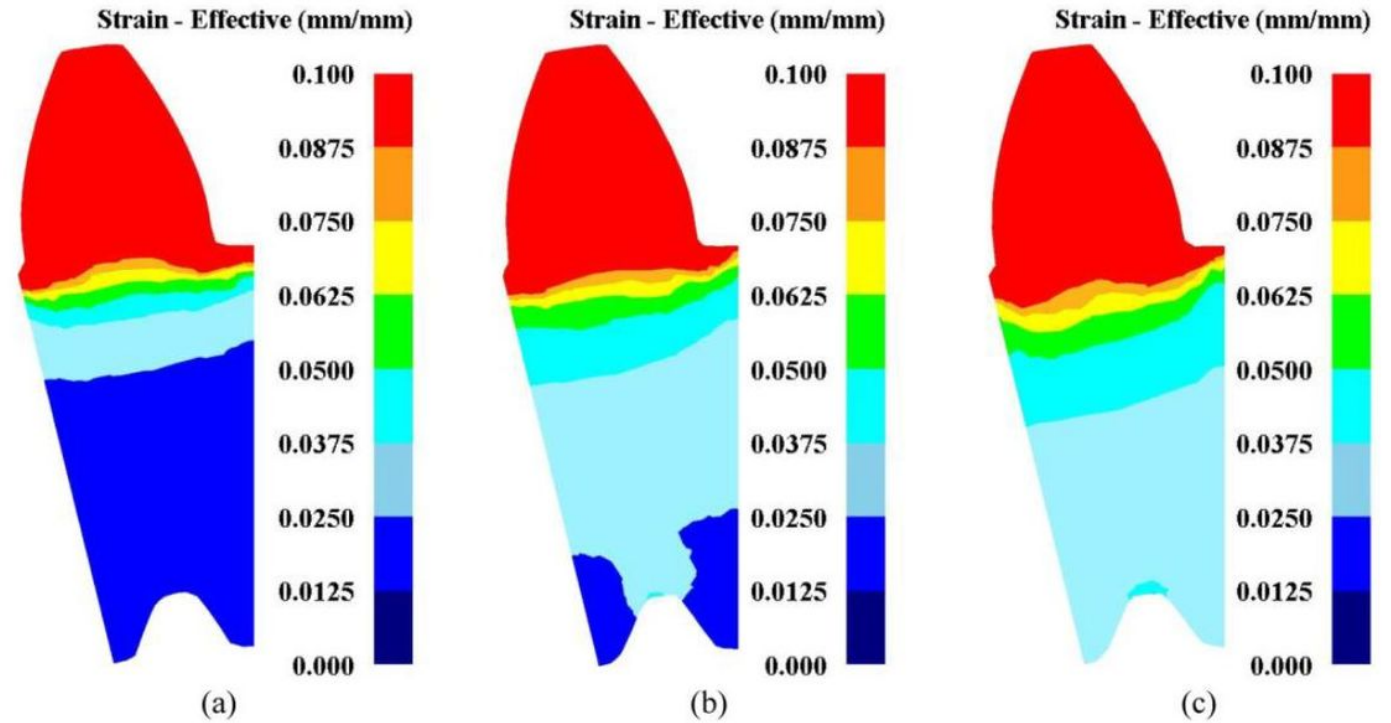

Figure 14

Effective stra in distributions of finished sun gear at different finishing tools: (a) mandrel with gap; (b) mandrel without gap; and (c) interference mandrel.

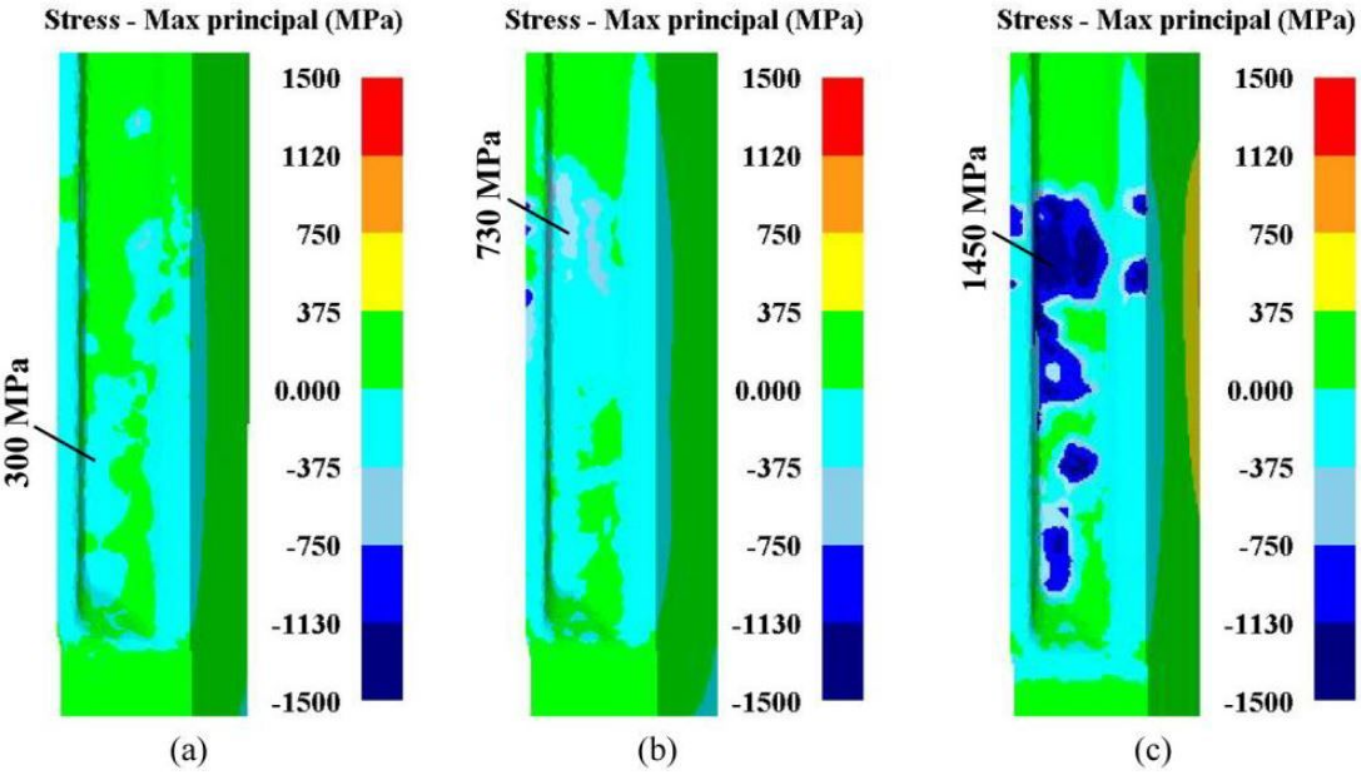

Figure 15

Max principal stress distributions of different spline mandrels: (a) mandrel with gap; (b) mandrel without gap; and (c) interference mandrel.

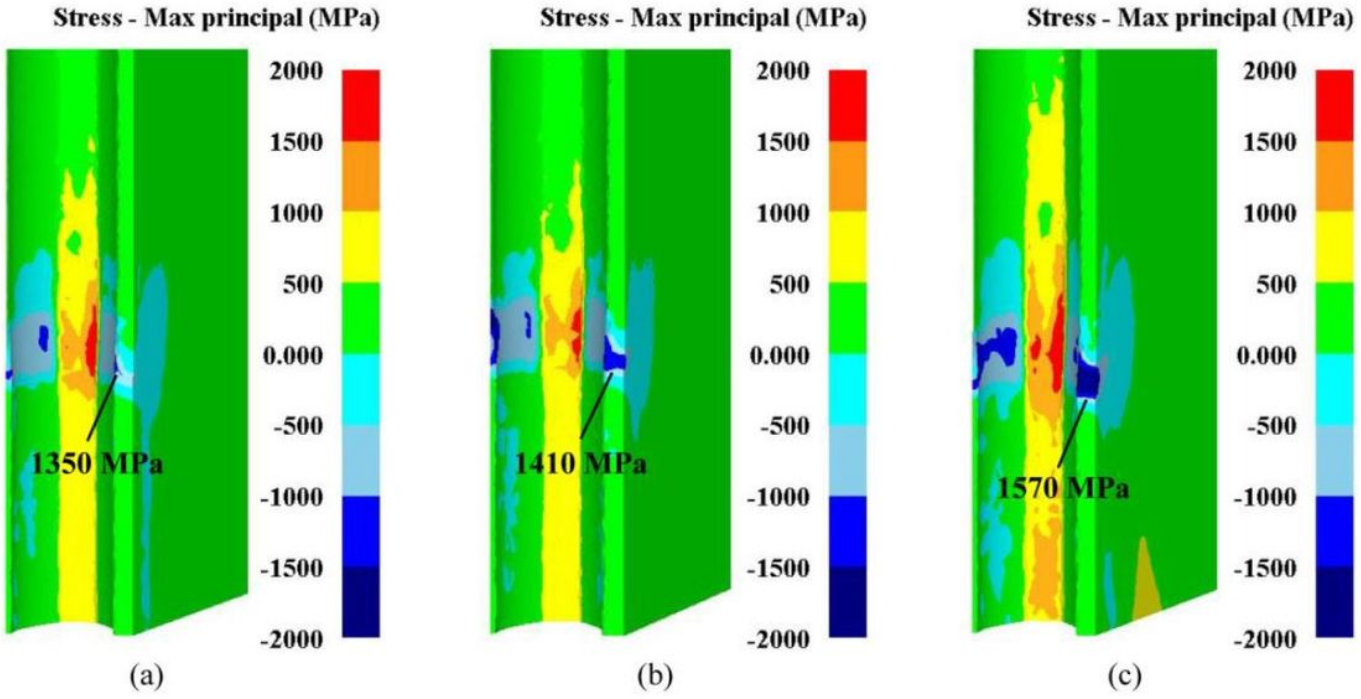

Figure 16

Max p rincipal stress distributions of toothed die at different finishing tools: (a) mandrel with gap; (b) mandrel without gap; and (c) interference mandrel.

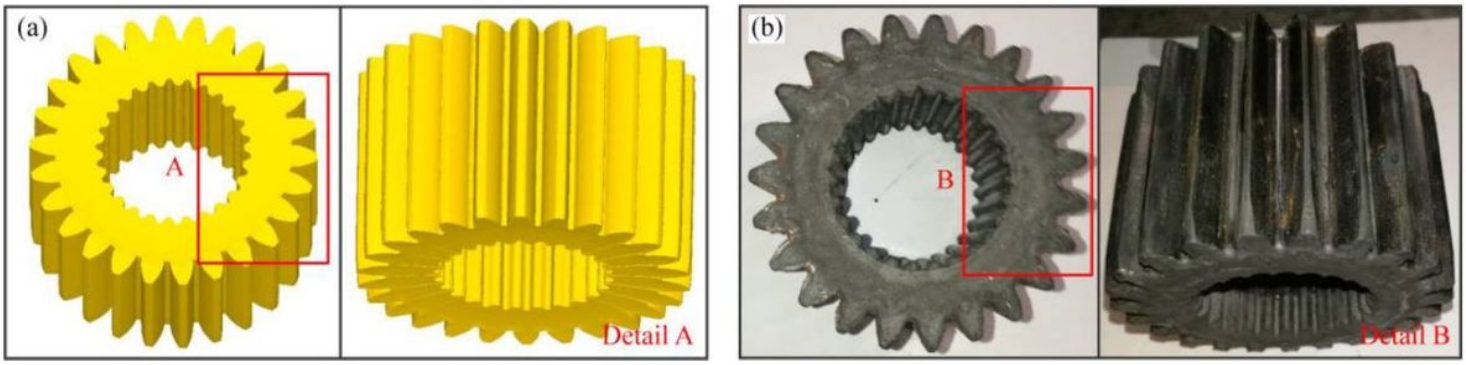

Figure 17

Results of precision finishing process: (a) FE simulation; and (b)

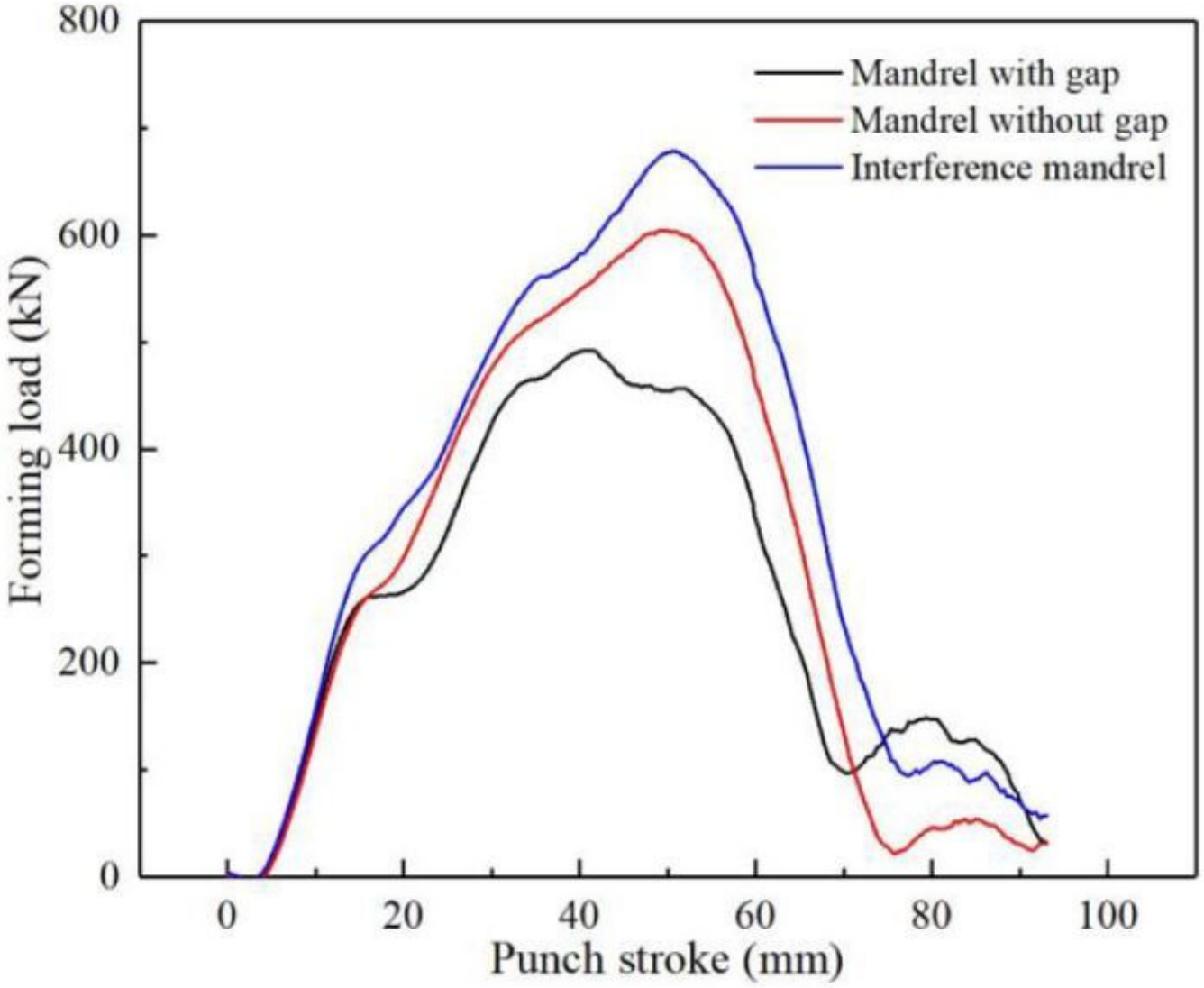

Figure 18

Forming load curves at different finishing tools

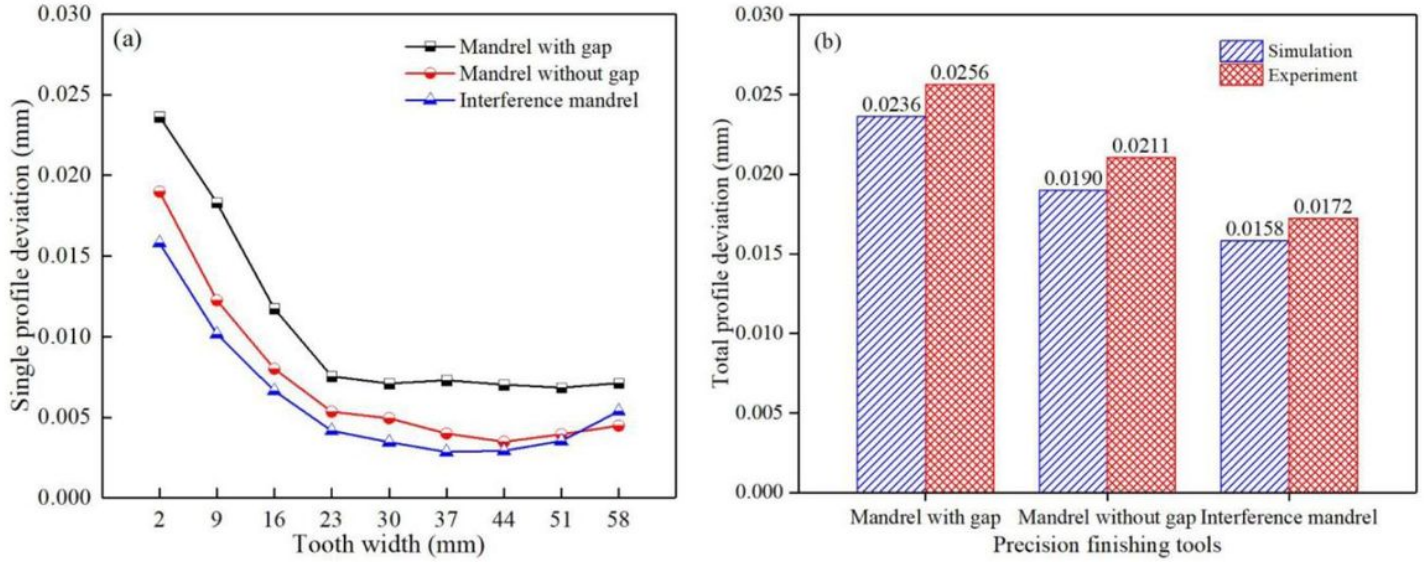

Figure 19

Profile deviations of external gear at different finishing tools: (a) single profile deviation; (b) total profile deviation.

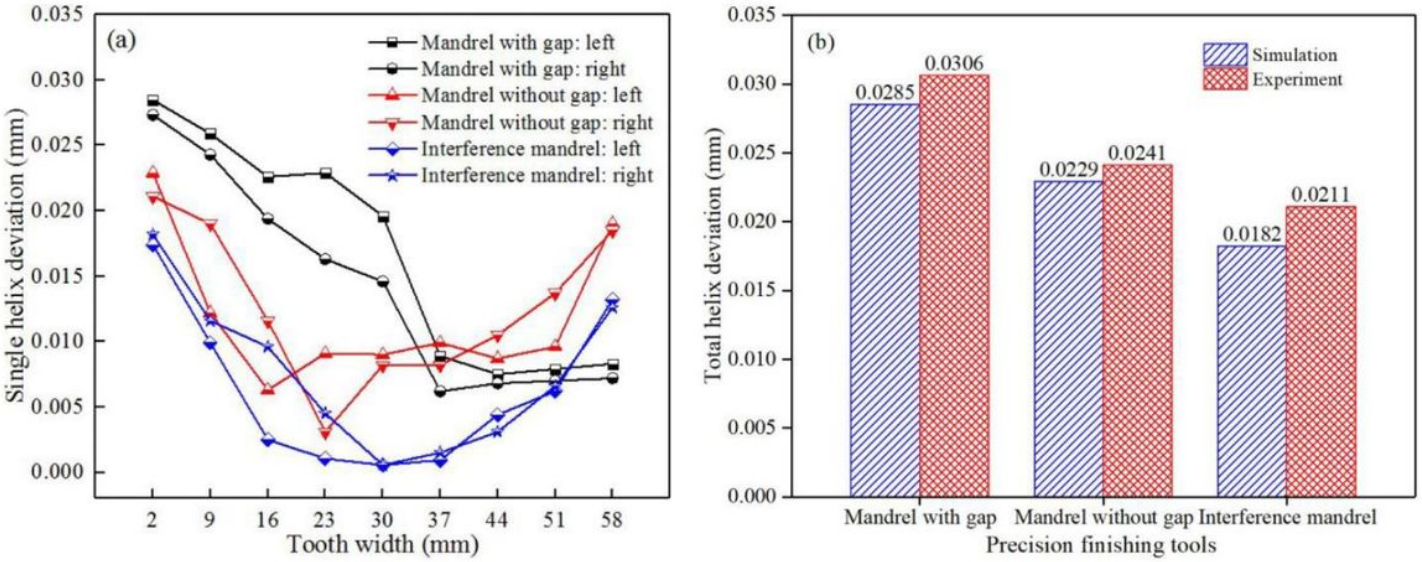

Figure 20

Helix deviations of external gear at different finishing tools: (a) single helix deviation; (b) total helix deviation.

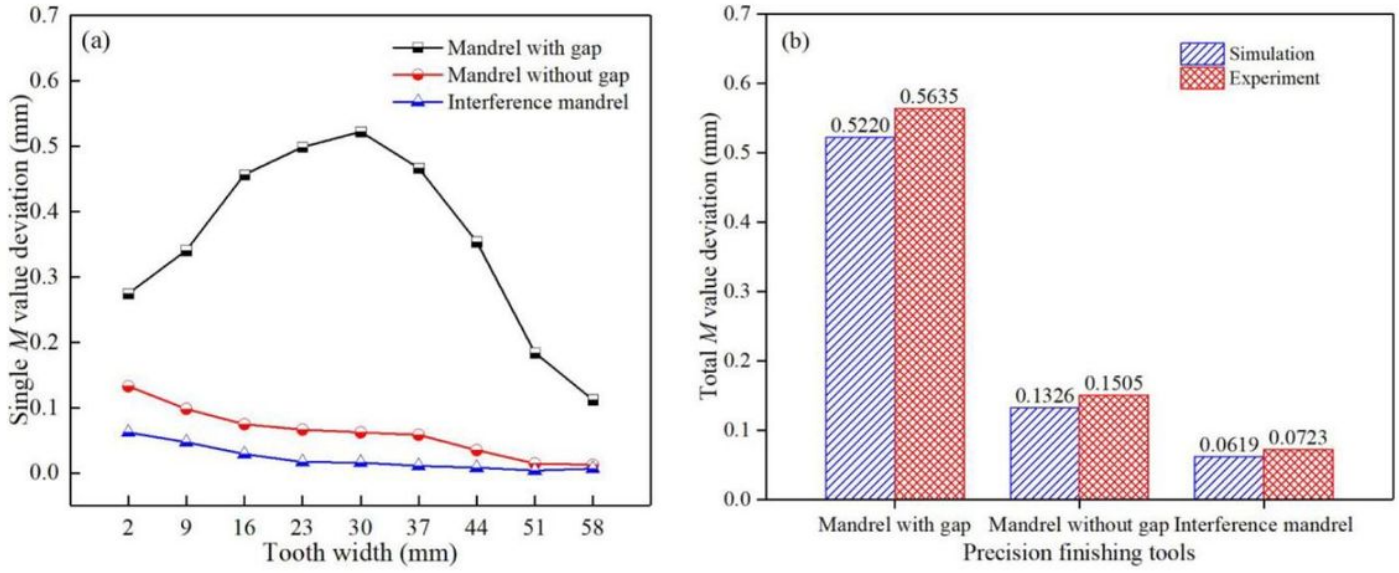

Figure 21

M value deviations of internal spline at different finishing tools: (a) single M value deviation ; (b) total M value deviation.

Supplementary Files

This is a list of supplementary files associated with this preprint. Click to download.

- Graphicalabstract.pdf